Masters Program in Geospatial Technologies

LAND COVER MAPPING WITH RANDOM FOREST USING INTRA-ANNUAL SENTINEL 2 DATA IN CENTRAL PORTUGAL

A COMPARATIVE ANALYSIS

Daria Lüdtke

Dissertation submitted in partial fulfilment of the requirements for the Degree of *Master of Science in Geospatial Technologies*

NOVA IMS Information Management School
Universitat Jaume I
Westfälische Wilhelms-Universität Münster

Land cover mapping with Random Forest using intra-annual Sentinel-2 data in Central Portugal

A comparative analysis

Dissertation supervised by

PhD Roberto Henriques

Professor, Nova Information Management School

University of Nova – Lisbon, Portugal

PhD Mário Caetano

Professor, Nova Information Management School

University of Nova – Lisbon, Portugal

PhD Carlos Grannell

Professor, Universitat Jaume I – Castellón, Spain

February 2018

ACKNOWLEDGMENTS

I would like to thank first my supervisor and co-supervisors Roberto Henriques, Mário Caetano and Carlos Granell. Their support and guidance in the realization of this research was indispensable.

I also leave my most sincere gratitude to the professors Joaquín Huerta, Michael Gould, Marco Painho, Christoph Brox, and Christian Kray for the organisation of the Master of Science in Geospatial Technologies and the support they gave to us students over the course of the degree. I would also thank all professors involved in the program for sharing their knowledge.

A special thank you goes out to Hugo Costa, formerly employed at the DGT in Lisbon, who gave a lot of his valuable time to support me with the methodology and critical input to my work. It was a pleasure to work with you.

My appreciation also goes to NOVA IMS, who supported my journey with a scholarship for the last semester.

My classmates also deserve my gratitude, since they made this experience what it was. I am glad to call you my friends, and I hope to share more memories with you in the future. A special shout out to Mr. Chaplin Williams, who was my closest ally and working mate. I can't imagine this journey without, and I am more than grateful for your presence and all the things I learned from you.

A final thank you to my friends and family, who were very supportive throughout the experience.

ABSTRACT

In recent years, data mining algorithms are increasingly applied to optimise the classification process of remotely sensed imagery. Random Forest algorithms have shown high potential for land cover mapping problems yet have not been sufficiently tested on their ability to process and classify multi-temporal data within one classification process. Additionally, a growing amount of geospatial data is freely available online without having their usability assessed, such as EUROSTAT´s LUCAS land use land cover dataset.

This study provides a comparative analysis of two land cover classification approaches using Random Forest on open-access multi-spectral, multi-temporal Sentinel-2A/B data. A classification system composed of six classes (sealed surfaces, non-vegetated unsealed surfaces, water, woody, herbaceous permanent, herbaceous periodic) was designed for this study. Ten images of ten bands plus NDVI each, taken between November 2016 and October 2017 in Central Portugal, were processed in R using a pixel-based approach. Ten maps based on single month data were produced. These were then used as input data for the classifier to create a final map. This map was compared with a map using all 100 bands at once as training for the classifier. This study concluded that the approach using all bands produced maps with 11% higher, yet overall low accuracy of 58%. It was also less time-consuming with about 5 hours to over 15 hours of work for the multi-temporal predictions. The main causes for the low accuracy identified by this thesis are uncertainties with EUROSTAT´s Land Use/Cover Area Statistical Survey (LUCAS) training data and issues with the accompanying nomenclature definition. Additional to the comparison of the classification approaches, the usability of LUCAS (2015) is tested by comparing four different variations of it as training data for the classification based on 100 bands.

This research indicates high potential of using Sentinel-2 imagery and multi-temporal stacks of bands to achieve an averaged land cover classification of the investigated time span. Moreover, the research points out lower potential of the multi-map approach and issues regarding the suitability of using LUCAS open-access data as sole input for training a classifier for this study. Issues include inaccurate surveying and a partially long distance between the marked point and the actual observation point reached by the surveyors of up to 1.5 km. Review of the database, additional sampling and ancillary data appears to be necessary for achieving accurate results.

KEYWORDS

Data Mining

Land Cover Classification

Multi-temporal classification

Open Access

R

Random Forest

Remote Sensing

Sentinel-2

Time-Series

ACRONYMS

BOA - Bottom-Of-Atmosphere

DGT - Direção-Geral do Território

EO – Earth Observation

ESA – European Space Agency

EUROSTAT - Statistical Office of the European Commission

L1C – Level-1C

L2A – Level-2A

LCC – Land Cover Classification

LUCAS - Land Cover/Use Statistics

LULC – Land Use Land Cover

MMU – Minimum Mapping Unit

MSI – Multispectral Instrument

NDVI – Normalised Difference Vegetation Index

OA – Open-Access

RF – Random Forest

S2 – Sentinel-2

SNAP - Sentinel Application Platform

TOA – Top-Of-Atmosphere

INDEX OF THE TEXT

INDEX OF TABLES

INDEX OF FIGURES

1. INTRODUCTION

This chapter will introduce the theoretical framework and motivation of the thesis in **Chapter 1.1**, state the objectives and aims in **Chapter 1.2**, and gives a general outline of the work in **Chapter 1.3**.

1.1. Theoretical Framework and Motivation

Remotely sensed imagery has established itself as the main source of information to determine land use and land cover. Simultaneously, satellite-based sensors continue to deliver data products of increasing temporal, spatial, and spectral resolutions. This allows for the development of new, more effective approaches to conduct remote pattern recognition in remotely sensed imagery. A wide variety of machine learning algorithms are now supporting and conducting classifications (e.g. Jia et al., 2014; Schmidt et al., 2014; Neves et al., 2015). Random Forest (RF) has established itself as a popular machine learning algorithm in the field (e.g. Gislason et al., 2006; Pal, 2005; Stepper et al., 2015). This is based on its high accuracy and speed, non-parametric approach to classification, and its ability to handle high data dimensionality while being insensitive to overfitting (Belgiu and Dra, 2016). Furthermore, it can be used with categorical, unbalanced, and incomplete data while still achieving high classification accuracy, which is not possible with other classifiers such as support vector machines (Pal, 2005).

Random Forest algorithms have shown high potential for land cover land use (LULC) mapping problems on multi-temporal, multi-spectral satellite data for LULC classification and change detection (e.g. Pelletier et al., 2016; Schneider, 2012; Yin et al., 2014). Nonetheless, the classifier has not been sufficiently tested on its ability to process and classify multi-temporal data within one classification process on a large scale by comparing different approaches.

This study provides a comparative analysis of two land cover classification approaches at pixel level. It aims at testing alternatives for processing multi-temporal data within one classification process. Specifically, it is using RF on open-access

multi-spectral, multi-temporal Sentinel-2A/B imagery of Central Portugal. The predictions made, their accuracies and the computational effort will be compared. For that, ten images of ten bands each were used. The images were taken between November 2016 and October 2017. A classification system composed of six land cover classes was designed (sealed surfaces, non-vegetated unsealed surfaces, water, woody, herbaceous permanent, herbaceous periodic). The first approach consisted of using all input variables from the 10 images plus NDVI at the same time in the classification process. The second approach consisted first of the production of ten land cover maps (one for each month) and then of the classification of these ten maps to generate a single map. All classifications were conducted with Random Forest.

The Normalised Difference Vegetation Index (NDVI) was calculated to estimate the vegetation´s photosynthetic activity in the area based on the single month data. This approach is common in optical time series analysis (Alcantara et al., 2012; Esch et al., 2014; Zhang et al., 2003). The index was subsequently used as an additional band in the single month land cover classification process to improve classification accuracy by differentiating classes with different types of vegetation (Steidl, 2017). The aforementioned approach has been successfully applied using MODIS and Landsat data and improved classification accuracy (Jia et al., 2014; Nitze et al., 2015).

This study is using Sentinel-2A/B (S2) data as imagery for the analysis. Sentinel-2 is provided online by the European Space Agency as an open-access product since 2015, providing imagery of high spatial and temporal resolution (imagery of 10m resolution and a temporal resolution of 5 days). Many studies available thus worked with simulated S2 data to assess its potential and uniformly came to positive conclusions of its potential (Clark, 2017; Dong et al., 2015; Drusch et al., 2012; Malenovský et al., 2012; Ramoelo et al., 2015; Van der Meer et al., 2014). Since the data is available, studies with S2 data cover a vast range of geographic issues. They include the assessment of burn severity (Fernández-Manso et al., 2016), classification exercises to map crop types and tree species (Immitzer et al., 2016), mapping water bodies (Du et al., 2016), monitoring fine-scale habitats (Stratoulias et al., 2015), discriminating forest types (Vaglio Laurin et al., 2016), and forest fire evaluation (Navarro et al., 2017). All studies see high potential in S2 data.

Additional to the assessment of the classification approaches, the usability of EUROSTAT´s Land Use/Cover Area Statistical Survey (LUCAS) database from 2015

is tested. This database contains land cover land use information of the EU member states as point data. It is aimed to find out if LUCAS is an alternative to selecting training areas for RF by photointerpretation and identify uncertainties and limitations. This is done by running the classification based on 100 bands on 4 different modifications of LUCAS: An unmodified version, one with added samples to balance unbalanced training data, and two with added samples and modifications of the class representing woodlands. The difference between the latter two is in the inclusion of a specific set of points manually added to help the classifier distinguishing dark forest canopy and water. The modifications on the class representing woodlands are based on results and issues found during the comparison of classifications approaches, yet are also designed to identify potential difficulties caused by the composition of the nomenclature. The rationale behind the dataset comparison is to assess the usability of LUCAS and to which extend it can be used to reduce the time usually associated with selecting training areas by photointerpretation while still achieving acceptable accuracies. It is hypothesized that additional sampling and extensive data pre-processing is needed in order to obtain results with high accuracy with LUCAS in this specific study.

Esch et al. (2014) is an exemplary study using RF with LUCAS point data both for training and evaluation of their classifier. The study aimed to differentiate cropland and grassland. Other studies using LUCAS data include soil erosion modelling (Panagos, et al., 2014), soil pH mapping (Gardi and Yigini, 2012) and land use land cover mapping (Mack et al., 2017). All aforementioned studies support their use of the LUCAS database with ancillary data from specialised databases or conducted extensive additional sampling.

For testing, a set of equalised stratified random points produced in ArcGIS was used. It is composed of 50 accuracy assessment samples per class. The samples are based on corresponding classes in the CORINE Land Cover Map 2012. To ensure the land cover has not changed since then, the 300 samples were controlled using visual inspection of 2017 EO imagery. The accuracy of the results is assessed using reference data bases consisting of samples (e.g. Gong et al., 2013; Inglada et al., 2015; Novelli et al., 2016) and visual inspection (e.g. Chen et al., 2005; Im et al., 2007; Van der Meer et al., 2014; Li et al., 2016).

1.2. Objectives and Aims

This study aims at answering two research questions:

1. How do the classification approaches perform on multi-temporal, multi-spectral data in general and compared to each other?
2. How usable is LUCAS data as training data for Random Forest and is it an alternative to selecting training areas by photointerpretation?

For answering the questions, the accuracy of the predictions of both classification approaches and four training data variations all outcomes are assessed. Uncertainties and limitations are identified and discussed, and suggestions to counterbalance these uncertainties are given.

The study is almost entirely based on open-source (OS) software and data with a focus on processing Sentinel-2 (S2) data products in R. The objectives and methodology used to answer the research questions can be summarised as follows:

Basic objective	*Related basic process and tools*	*Optimised process*
Process Sentinel 2 imagery to usable product	**Process Level-1C to Level-2A data products using Sentinel´s Sen2Cor in Sentinel Application Platform**	Process Level-1C to Level-2A data products using Sen2Cor as batch in Windows Command Prompt
	Conversion of JP2 to GeoTIFF	Conversion of JP2 to GeoTIFF with GDAL Scripts using USGS Raster Conversion Scripts
Process LUCAS data to train classifier	**Process LUCAS 2015 point data in R (cropping and outlier removal) and ArcGIS (additional sampling and cleaning)**	
Use additional indices or index to contribute to classification accuracy	**Calculate NDVI in R for extra information for the classifier**	Calculate NDVI band as additional information for the classifier and use it as threshold to assign classes in nomenclature
Design transferable nomenclature	**Identify transferable classes in the nomenclatures**	
Classification of land cover map based on monthly maps	**Creating code for RF classification based on single month maps in R**	

Classification of land cover map based on all bands	**Creating code for RF classification based on all bands in R**
Comparison and evaluation of classification approaches	**Creation of random stratified sampling points in ArcGIS**
	Accuracy assessment of the final maps in R using statistics
	Identification of differences in class size and pixel distribution and identifying causes
Evaluation of LUCAS data suitability	**Statistical evaluation of database products**

Table 1. Basic objectives and basic and optimised processes

Table 1 shows the basic objectives in the left column. The related basic processes are displayed in the middle column. The optimisation of the process, if available, is described in the right column. Otherwise it is left blank.

1.3. Outline

The structure of the remainder of the document is as follows: **Chapter 2** contains the literature review. It describes the related work previously done in the field, providing background knowledge to this thesis. **Chapter 3** presents the data and the study area. **Chapter 4** discusses the approach, tools and the methodology that has been used. **Chapter 5** presents and discusses results obtained in the thesis. **Chapter 6** concludes the project, highlights its contributions and then provides suggestions for further research in the area.

2. LITERATURE REVIEW

This Chapter will provide an overview on the literature relevant for the study. The topics covered are land cover classification (multi-spectral and multi-temporal) in **Chapter 2.1**, Sentinel-2 Multispectral Instrument (MSI) data products in **Chapter 2.2**, the use of LUCAS data in present literature in **Chapter 2.3**, the use of Random Forest for land cover classification in **Chapter 2.4** and definition and review of the accuracy assessment tools in **Chapter 2.5**.

2.1. Introduction to Land Cover Classification

A main application in terrestrial remote sensing data is the analysis and classification of land cover. Land cover is always dependent on the study area and includes different classes, such as water, urban areas, and different types of forests and crops. It is a basic variable with high significance for assessing the environment (Foody, 2002). Therefore, accurate and relevant information on land cover are increasingly in demand in many areas of government, economy and science (Homer et al., 2007). Due to the range of applications, thematic maps are thus needed in a variety of temporal and spatial resolutions. Applications include change detection (Singh, 1989), habitat mapping (Schuster et al., 2015; Stow et al., 2008), agriculture (Blaschke, 2010; Deren et al., 2003; Lu et al., 2013), disaster risk management (van der Sande et al., 2003), and vegetation mapping (Karlson et al., 2015; Vaglio Laurin et al., 2016).

Multi-temporal classification is one approach for land cover classification (LCC). It is based on using imagery acquired over a specific time period ranging from several weeks to multiple years for classification. With the steady increase in spatial, spectral and temporal resolution, these classifications now include a multitude of bands on a high spatial resolution of a few meters. This leads to a high dimensionality of data and new challenges in the field.

Pelletier et al. (2016) (which will also be discussed in **Chapter 2.4**) successfully used Random Forest as a classifier on multi-temporal, multi-spectral satellite imagery. The study is using different tiles of Landsat-8 and SPOT-4 images

to simulate S2 data with an average temporal resolution of 13 days from April 2013 until November 2013. An overall accuracy of over 80% was documented. The study concludes that the classifier is able to identify both static land cover types, such as forestry, and dynamic land cover types, such as agriculture.
The study states that RF was able to sufficiently discriminate land cover types by exploiting the temporal information of the spectral signatures alone, though a slight increase in the classification accuracy of dynamic land cover types is indicated. The reportedly small increase in accuracy when using ancillary data is outweighed with a significantly increased computational time.

Yin et al. (2014) ran a similar study of mapping annual land use and land cover changes using a MODIS time series. This particular study also uses RF as the classifier on a pixel-based approach. Based on MODIS VI data, a 16-day product of 250m spatial resolution, they used all available imagery between mid-February of 2000 and December 2001 of a region in Inner Mongolia. The nomenclature used for this study was very similar to the one used in this study, consisting of six land use and land cover classes. These include cropland, forest, grassland, constructed area, water, and bare lands. The study achieved an overall mapping accuracy of 92%. The main uncertainties stated were the confusion between very low vegetated grassland and permanent non-vegetated areas and the confusion between croplands and grasslands. The first uncertainty is explained by the high temporal variance of rainfall and similarities in spectral values. The second uncertainty is caused by similar spectral and temporal patterns of the land cover classes, which makes it difficult to differentiate them solely based on remote sensing data. To achieve high accuracy, the study used both homogenous and heterogenous testing samples to suggest mixed-land cover. The study is concluded highlighting the potential of trajectory-based methods for LULC mapping, specifically to detect land use changes.

Multi-temporal, multi-spectral imagery is also used by Schneider (2012). The study used a variety of machine learning algorithms, one being RF, on 35 to 50 Landsat scenes and NDVI as input bands for three study areas in China for urban change detection. Though achieving good results of 74.6% to 89.4% overall accuracy with RF, the study points out the importance of seasonal information since classes such as bareland, uncultivated or fallow agriculture and new construction sites can

easily be confused by the classifier. Other limitations discussed are the computational effort needed to process these large quantities of data and the availability of cloud-free data.

A topic repeatedly discussed for multitemporal studies is the question how single or multiple data acquisition dates affect the classification accuracy (Schmidt et al., 2014; Schuster et al., 2015). Esch et al., 2014 successfully attempted in his study to reduce the effect of specific weather and soil conditions by approximating a general class description for agricultural crops using multi-temporal satellite data. Also Nitze et al. (2015) recognised the positive effect multi-temporal classification can have on classification accuracies.

In conclusion, multi-spectral and multi-temporal data as input for land cover classifications showed high potential, yet are subject to a variety of limitations. These range from financial to the need of large amounts of imagery taken under good atmospheric conditions. The need of remotely sensed time series imagery to cover large areas at high spatial and temporal resolution without becoming too costly was difficult to meet in many studies discussed (e.g. Wardlow and Egbert, 2008). A common trade-off in remote sensing studies is to either chose high spatial or high temporal resolution data (Lambin and Linderman, 2006). Nevertheless, the use of multi-temporal satellite data, especially to classify vegetation, has increased with the improvement of spatial and temporal resolutions of satellite capabilities (Atzberger and Eilers, 2011; Justice and Hiernaux, 1986; Zhang et al., 2003). A recent development in this field was the shift from using relatively spatial coarse data products (250 m to 1 km) from optical sensors such as, TERRA MODIS, ENVISAT MERIS or SPOT VEGETATION (Atzberger and Eilers, 2011; Gu et al., 2010; Jia et al., 2014; Lu et al., 2013; Neves et al., 2015; Nitze et al., 2015; Zhang et al., 2003) to using data products obtained by multi-sensor satellite systems such as RapidEye or Sentinel-2A/B, who provide data products of strongly increased resolutions (Schuster et al., 2015).

2.2. Sentinel-2 Data in Present Literature

Not only the technology to acquire the data and its resolutions have been steadily improving, but also its availability. Institutions such as the European Union have committed to an open-access agenda to make data freely available to the public. This development is part of the Big Free Data movement in remote sensing. Sentinel-1A/B as part of the European Copernicus program and Landsat-8 as part of the Landsat project were especially contributing to create freely available data on a regular basis (Kussul et al., 2017).

Two of the most recent additions to sensors creating freely available Earth Observation (EO) data in high resolution were the launches of Sentinel-2A in June 2015 and Sentinel-2B in March 2017 (ESA, 2017a). The twin satellites will share the orbit 180° apart from each other, thus increasing the temporal resolution of products available. With both satellites orbiting, the temporal resolution reached five days (Wang et al., 2016). The Sentinel-2 satellite imagery has been made freely available by the European Commission's Copernicus program to further research and monitoring. The Multispectral Instrument (MSI) with a swath width of 290 km produces high-resolution imagery with 13 spectral bands (443 nm–2190 nm) available every five days. The spatial resolutions available are 10m (4 visible and near-infrared bands), 20m (6 red-edge/shortwave-infrared bands) and 60m (3 atmospheric correction bands) (Drusch et al., 2012).

Three types of data products are offered on the homepage of the European Space Agency (ESA), which is hosting the Sentinel-2 data: Level-1B products which consist of sensor geometry of top-of-atmosphere radiances. Level-1C products which consist of top-of-atmosphere (TOA) reflectances in a combined UTM projection and WGS84 ellipsoid. And lastly Level-2A products which are bottom-of-atmosphere (BOA) reflectances in a cartographic geometry (ESA, 2017). The product used for this thesis are Level-2AC and Level-1C data products. The latter needs to be processed and formatted to L2A with Sen2Cor (ESA, 2017c; ESA, 2017d), a processor correcting atmospheric effects to produce L2A surface reflectance data (Louis et al., 2016).

All studies based on Sentinel-2 are fairly new since the satellite has only been in orbit since 2015. Therefore, many studies available are based on simulated MSI data to assess the potential of S2 data. Applications range from geological mapping to

water body modelling (Clark, 2017; Dong et al., 2015; Drusch et al., 2012; Malenovský et al., 2012; Ramoelo et al., 2015; Van der Meer et al., 2014). For example, Clevers and Gitelson (2013) positively assessed the usability of the red-edge bands of Sentinel-2 as the basis for calculating vegetation. All studies concluded to see high potential in the data derived from the sensor due to its high spatial and temporal resolution.

The selection of scientific papers using actual S2 MSI data in their studies is relatively limited. Fernández-Manso et al. (2016) successfully used S2 data for burn severity, calling the data adequate for this type of study. Classification exercises to map crop types and tree species with Sentinel-2 data by Immitzer et al. (2016) supported this outcome. Other applications include mapping water bodies (Du et al., 2016), monitoring fine-scale habitats (Stratoulias et al., 2015), discriminating forest types (Vaglio Laurin et al., 2016), and forest fire evaluation (Navarro et al., 2017). All studies see high potential in S2 MSI data.

On the subject of whether S2 data differs in usability from other high-resolution sensor products such as Landsat 8, results of studies differ. In a study of 2016, Novelli et al. conducted a performance evaluation test comparing S2 data and Landsat 8 Operational Land Imager data based on their ability to perform object-based greenhouse detection. Both Kappa Index of Agreement and Overall Accuracy of the study indicated that S2 predictions performed consistently better than the corresponding Landsat 8 predictions. This result was attributed to the better performance of S2 features in the RF classification training process. It was concluded that these results indicate S2 as the more stable data source to efficiently extract greenhouses irrespective of atmospheric conditions. On the other hand, Korhonen et al. (2017) found no systematic differences between Landsat 8 and Sentinel-2 in their study on estimating boreal forest canopy cover and leaf area index.

In conclusion, Sentinel-2 data provides high usability for a multitude of applications in the remote sensing field by providing data products of global coverage, fine spatial resolution and relatively fine temporal resolution (Wang et al., 2016).

2.3. LUCAS Data in Present Literature

The data used as ground truth was extracted from LUCAS micro-data for Portugal, an OA spatial database[1]. LUCAS is a geographical in-situ survey conducted every three years since 2000 by the Statistical Office of the European Commission (EUROSTAT) to detect land cover and land use (LULC) changes in the European Union-28 territory (EC, 2017). The point database consists of detailed land cover and land use attributes for large parts of Europe accompanied by respective ground truth photographs (Karydas et al., 2015).

Its primary goal is to provide multi-temporal, comparable statistical information about the participating countries (Karydas et al., 2015). Moreover, it is used to monitor the implementation of the Europe 2020 strategy by providing the data used to calculate agro-environmental indicators, sustainable development indicators and land take. Additionally, it is used for production, verification and validation of land cover mapping initiatives such as Copernicus' CORINE Land Cover (EUROSTAT, 2016).

LUCAS classification is composed of eight main categories indicated by capital letters: A: Artificial land; B: Cropland; C: Woodland; D: Shrubland; E: Grassland; F: Bare land; G: Water areas; H: Wetlands. These main categories are further divided into a total of 76 subclasses. These classes are defined by the combination of the letter of the main class and two to three digits (Karydas et al., 2015).

The sampling process of LUCAS data is conducted in two phases. In the first phase, the territory is covered with a 2x2 km grid to obtain the LUCAS master, containing around 1.100.000 points in Europe. These points are then categorised by photointerpretation of aerial imagery. In the second phase, n out of N points are selected per class and visited in-situ to conduct a more detailed LCLU survey. It is a combined approach of photointerpretation and in-situ information collected during groundwork (EUROSTAT, 2016).

Literature of studies based on LUCAS data are not common. Esch et al. (2014) used LUCAS data for training and evaluation of their classification. The study used an object-based approach to distinguish cropland and grassland in an area of 15km by

[1] http://www.eea.europa.eu/data-and-maps/explore-interactive-maps/changing-face-of-europe-2014#tab-based-on-data Last access: 20.02.2017

15km using multi-spectral, multi-seasonal imagery. It resulted in an overall accuracy (OA) of 86% and a Kappa coefficient of 0.79. A land use land cover mapping approach by Mack et al. (2017) based on the LUCAS points achieved overall high accuracy levels with above 85% for most classes and an overall accuracy of 87%. Nonetheless the study´s suggestions for future work include to concentrate on efficient ways to minimise the quantity of unsuitable LUCAS data for LCC. Both studies also observed imbalanced training data. Other studies using LUCAS data include soil erosion modelling (Panagos et al., 2014), and soil pH mapping (Gardi and Yigini, 2012). It is important to note that all aforementioned studies support their use of the LUCAS database with ancillary data to increase classification accuracy.

Another set of studies used the LUCAS data as reference data for validating large-scale LULC maps based on remotely sensed imagery (Gallego, 2011; Karydas et al., 2015)**.** Karydas et al. (2015) used a comparative approach to determine the suitability of LUCAS data as a reference dataset to validate a Land Cover Map of Greece for 2007. He compared an "automated" classification process entirely relying on the LUCAS main land cover attribute to a "supervised" classification process, where the classification was based on photointerpretation of LUCAS imagery. The automated classification approach resulted in an accuracy of 61.9% while the supervised approach resulted in an accuracy of 51.8%. The study found the database to be supportive yet limited in efficiency to verify the Land Cover Map used in the study. Two of the main issues raised were misclassifications of samples by LUCAS surveyors and that many points were assigned a class from distance and had to be removed from the study. In this particular case, 23.7% of all points used were excluded from assessment. In conclusion, the study suggested that LUCAS could rather be used as a verification than a validation dataset. Similar issues were raised by Gallego (2011), whose study validated then-available EU reference data. This study resulted in 67.3% estimated overall accuracy before increasing the accuracy to 75% by excluding a class from the assessment. Unlike Karydas et al. (2015), this study does not advise against using LUCAS as validation data for land cover maps. Still it states that automatic processing of this data is often insufficient for validation and recommends photointerpretation of the ground truth photography included in the database.

Nonetheless, little experience exists in using LUCAS data as the sole input for large-scale LCC. Mack et al. (2017) stated that a specific issue to investigate is the usability of LUCAS data as a training data base for supervised classification approaches, which is one of the two aims of this study.

2.4. The Use of Random Forest for Land Cover Classification

In the last two decades, machine learning algorithms for LCC have been increasingly used and adapted by the scientific community (Lawrence and Moran, 2015). One of the most popular and heaviest tested algorithms is RF, a machine learning ensemble producing a group of decision tree classifiers based on a bootstrapped training set of data (Breiman, 2001; Gislason et al., 2006; Pal, 2005). The most popular and thus final class is identified by having decision tree ensemble vote to achieve the highest accuracy (Breiman, 2001). Nitze et al. (2015) summed the requirements for this classifier up as:

"a reference dataset, containing numerical data (e.g. VI or reflectances) and its corresponding class label for the training of the classifier and its internal accuracy calculation." (p.5).

This classifier is widely and successfully used to perform classifications and regressions on remotely sensed imagery (e.g. Gislason et al., 2006; Pal, 2005; Stepper et al., 2015). It has been widely and successfully applied for regional land cover mapping using multi-temporal data (Alcantara et al., 2012; Fagan et al., 2015; Rodriguez-Galiano et al., 2012; Zhao et al., 2016) and multi-spectral data (Clark et al., 2012; Gessner et al., 2015; Lawrence and Moran, 2015; Rodriguez-Galiano et al., 2012b; Rodriguez-Galiano et al., 2012a; Zhao et al., 2016)**.**

Advantages for using RF for land cover mapping lay were mentioned in the theoretical framework of the thesis **(Chapter 1.1)**, yet can be summed up as follows: RF as a classifier provides high accuracy and speed in training and application, non-parametric approach to classification, and is able to handle high data dimensionality while being insensitive to overfitting (Belgiu and Dra, 2016). It can be used with categorical, unbalanced, and incomplete data and with little user input while still

achieving high classification accuracy, which is not possible with other many classifiers (Clark, 2017; Pal, 2005). As it is relatively insensitive to small sample size relative to its presence in the feature space, also known as *Hughes* effect, it is suitable for this study. Additionally, RF can be used to detect and rank variables with the highest ability to differentiate between targeted classes. This ability can be very useful and time-saving when working with highly dimensional data such as remotely sensed imagery (Neves et al., 2015). Moreover, by automating the ranking and selection of the most important variables, it makes the selection less subjective and error-prone (Belgiu and Dra, 2016; Belgiu et al., 2014).

A study which incorporates several elements also used in this study is Novelli et al. (2016). The study uses a combination of RF and multi-temporal, multi-spectral S2 data for greenhouse detection sand achieved overall accuracy values ranging from 87.9% to 93.4%.

Pelletier et al. (2016) discusses the use of RF and Support Vector Machines on high spectral, temporal and spatial resolution remotely sensed imagery (Landsat-8 and SPOT-4) as a time-series. The discussion indicates a set of challenges common when using machine learning algorithms for land cover classification: Firstly, to identify the correct classifier to handle the high resolutions and dimensionality of the data. Secondly, to evaluate how stable the classifiers are. Thirdly, how to select the most appropriate feature set for training the classifier while balancing accuracy of the classification and computational time needed. And fourthly, how to maintain classification accuracy over extensive areas. The study concludes with good results for both classifiers, though RF reached a slightly higher overall accuracy. Other studies, where RF provides better results than other classifiers confirm this conclusion (e.g. Schneider, 2012).

Moreover, additional advantages of RF are indicated. These include a small training time and easy parametrisation. Another relevant conclusion of the study is that the setting of parameters has little influence on the classification accuracy. These finding indicate that RF is a suitable algorithm for multi-temporal, multi-spectral classifications of large areas based on spectral bands like in this study.

2.5. Accuracy Assessment Tools

Choosing the most suitable accuracy assessment tools is an extensively researched and discussed topic in the field of remote sensing. Not all tools are appropriate for all studies, thus this chapter only discusses the ones applied in this thesis. As stated in the theoretical framework (**Chapter 1.1**), the accuracy of the results is assessed using reference data bases consisting of samples resulting in kappa coefficient of agreement, confusion matrices and overall, user, and producer accuracy (e.g. Gong et al., 2013; Inglada et al., 2015; Novelli et al., 2016). Additionally, this thesis relies on visual inspection (e.g. Chen et al., 2005; Im et al., 2007; Van der Meer et al., 2014; Li et al., 2016).

An often used tool in land cover classification assessment is an confusion or error matrix. It is describing the pattern of class allocation made by the classifier in relation to a reference data set. One of the measures to be derived from confusion matrices is the percentage of the samples which were correctly allocated, which is indicating the overall accuracy of the prediction. Unlike the kappa coefficient and other measures that can be derived from a statistical assessment of a classification, confusion matrices also make full use of the information content by giving more detailed information on the number of correctly and incorrectly classified samples per class (Congalton and Green, 1993; Congalton, 1991; Foody, 2002). It allows for the accuracy assessment to focus on individual classes. This is enabled by relating the amount of samples which were correctly allocated to the sum of samples in the class. Depending on if the calculations are based on the column or row marginals of the matrix, this results in the so called producer´s and user´s accuracy (Campbell, 1996).

The cross-tabulation of observed ground or reference data to a classified label has established itself as the foundation of accuracy assessment in remote sensing (Canters, 1997). It enables the description of classification accuracy and locate and characterise errors. This information can then be used to refine the classification or correctly assess the results and what they indicate. An example for this is if there is a high rate of confusion between two specific land cover classes in the matrix, ancillary data containing information for the classifier to discriminate the two could increase correct classifications. Moreover, it can help to identify misclassifications in a map

and thus give a more accurate idea of the area extent of land cover types. For example, if the confusion matrix helps identifying a class which has a high rate of being misclassified as another class, the extent of the first class seen on a map based on the same classification can be assumed to be higher than depicted (Hay, 1988; Jupp, 1989).

Though using confusion matrices as a tool for accuracy assessment is established and informative, the scope of accuracy assessment should not be limited to this metric (Congalton and Green, 1993). A major problem discussed in the literature is the possibility that the samples were coincidentally assigned to the correct class (Pontius, 2000). Cohen´s kappa coefficient is used as a standard metric to compensate for this effect. It was introduced by the scientific community into studies in a variety of scientific fields. It measures the rate of agreement or disagreement by chance and allows the calculation of a variance term. The significance of the difference between a set of coefficients can thus be calculated (Foody, 2002). A kappa value of 0 indicates an agreement that is equal to complete chance, while a kappa value of 1 indicates complete agreement (Viera and Garrett, 2005). This makes it an attractive metric for assessing classification accuracy.

Nonetheless, e.g. Foody (2002) discusses the kappa coefficient in a critical way. The study is stating that despite its popularity, its ability to compensate for change agreement in classifications and its ability to allow the evaluation of the differences in accuracy is not unique among the accuracy metrics. This disagrees with calls made in literature to establish the kappa coefficient as a standard measure (Smits et al., 1999).

3. STUDY AREA AND DATA

This Chapter will introduce the study area (**Chapter 3.1**) as well as the S2 and LUCAS datasets used (**Chapter 3.2.1** and **Chapter 3.2.2** respectively) to conduct the research. Moreover, the composition of the nomenclature will be discussed in **Chapter 3.2.2.** A detailed description of data processing will be provided in **Chapter 4**.

.

3.1. Study Area

The selection the study area was conducted by the *Direção-Geral do Território* (DGT- engl. *Directorate-General for the Territorial Development*) located in Lisbon, Portugal. One S2 tile of Portugal was chosen as the area of interest. The study region as presented in **Figure 1** is a 100km by 100km large area in Central Portugal. Located North-West of Lisbon, it includes the city of Santarém and land East of Santarém along the Tagus river. It was deemed most suitable for the study, since it is covered by a variety of land use and land cover types: According to CORINE Land Cover Map of 2012, the LC types include artificial surfaces (urban fabric, mineral extraction sites, etc.), a variety of types of agricultural areas, forest and semi natural areas, and waterbodies[2]. Especially because of its agriculture, the cyclic changes in the vegetation over course of a year were expected to be strongly reflected in the reassignment of samples according to their NDVI values. This adds an additional dimension to the analysis.

[2] CORINE Interactive Land Cover Map. http://www.eea.europa.eu/data-and-maps/explore-interactive-maps/changing-face-of-europe-2014#tab-based-on-data Last access: 20.01.2018

Figure 1. Study Area in Central Portugal (shapefile taken from DGT, 2017a)

3.2.Data

Two different data sets are used in this study: The S2 remotely sensed imagery of the study area and land cover point data extracted from the Eurostat Land Cover/Use Statistics (LUCAS) dataset of 2015 used to build and train the classifier.

3.2.1. Sentinel-2 Imagery

The S2 imagery was obtained free of charge from the Copernicus Open Access Hub[3], the online system of the ESA on 21.11.2017. The hub was established to make Sentinel products accessible to data users (Copernicus, 2017).

The S2 data products downloaded are 10 sets of 13 bands respectively, each representing the 10 000km^2 large site defined in **Chapter 3.1**. An overview of the data products used is in **Table 2**. The parameters to identify the appropriate products for the analysis were the following: a sensing period time frame of November 2016 to October 2017 and a cloud coverage percentage of up to 10%. Data could both be derived from S2A and S2B missions. The initial data format is JP2.

[3] Copernicus Open Access Hub (2018). Available at: https://scihub.copernicus.eu/dhus/#/home. Last access: 25.01.2018

Image number	Sensing date	Sensor	Downloaded data product
1	16.11.2016	S2A	Level-1C
2	26.12.2016	S2A	Level-1C
3	15.01.2017	S2A	Level-1C
4	05.04.2017	S2A	Level-1C
5	25.05.2017	S2A	Level-2A
6	14.06.2017	S2A	Level-1C
7	14.07.2017	S2A	Level-2A
8	18.08.2017	S2B	Level-1C
9	27.09.2017	S2B	Level-1C
10	27.10.2017	S2B	Level-1C

Table 2. Selected data products in overview

The data products selected are eight Level-1C (L1C) and two Level-2A (L2A) products. L1C data contains top-of-atmosphere reflectance values in a fixed cartographic geometry of combined UTM projection and a WGS84 ellipsoid (Zone 29 North). The L2A data preserves the cartographic geometry, yet contains bottom-of-atmosphere reflectance values (ESA, 2017b).

Unlike data products on lower levels (Level-1A and 1B), these products are radiometrically and geometrically corrected (including orthorectifications and spatial registrations) (ESA, 2017a). To work with the L1C tiles, an additional processing step was required: Through further corrections of atmospheric effects, they were converted to L2A products using the Sen2Cor processor (Louis et al., 2016). The Sen2Cor processor is a tool available in the S2 Toolbox developed for the ESA in the common Sentinel Application Platform (SNAP). It allows analysis, visualisation and processing of MSI data derived from the S2 missions. Processing to Level 2A products calculates bottom-of-atmosphere reflectances in the same cartographic geometry and conducts scene classifications and atmospheric corrections (ESA, 2017c; ESA, 2017d). Details of this process will be provided in **Chapter 4.3**.

The bands used for ground geometry were preselected for the research. Of the 13 bands available through the MSI on Sentinel-2 the following were used: 10m spatial resolution bands B2 (490nm), B3 (560nm), B4 (665nm), and B8 (842nm), and the 20 m spatial resolution bands B5 (705 nm), B6 (740 nm), B7 (783 nm), B8a (865nm), B11 (1610nm), and B12 (2190nm) (ESA, 2017b). The three bands with 60m spatial resolution (B1 (443nm), B9 (940nm), and B10 (137nm)) were each excluded from the analysis. This was done since their data was not useful for this study. Additionally, downscaling them to 10m resolution would drastically decrease the quality of data and output.

The 20m resolution bands were downscaled to 10m using the "raster" package in R (Hijmans et al., 2017). Therefore, the Minimum Mapping Unit (MMU) of this study is a pixel of 10m x 10m.

3.2.2. LUCAS Data and Nomenclature Composition

964 LUCAS points were available as ground truth in the study area selected. The records represented 43 sub-categories according to the LUCAS classification which were merged into their eight main land cover categories according to EUROSTAT (2017) (**Table 3**). The locations of the point features are visible in **Figure 2**.

LUCAS category	**Artificial land**	**Cropland**	**Woodland**	**Shrubland**	**Grassland**	**Bare land**	**Water**	**Salt marshes**
Sample size	50	194	471	79	137	17	14	2

Table 3. Original LUCAS nomenclature and sample distribution

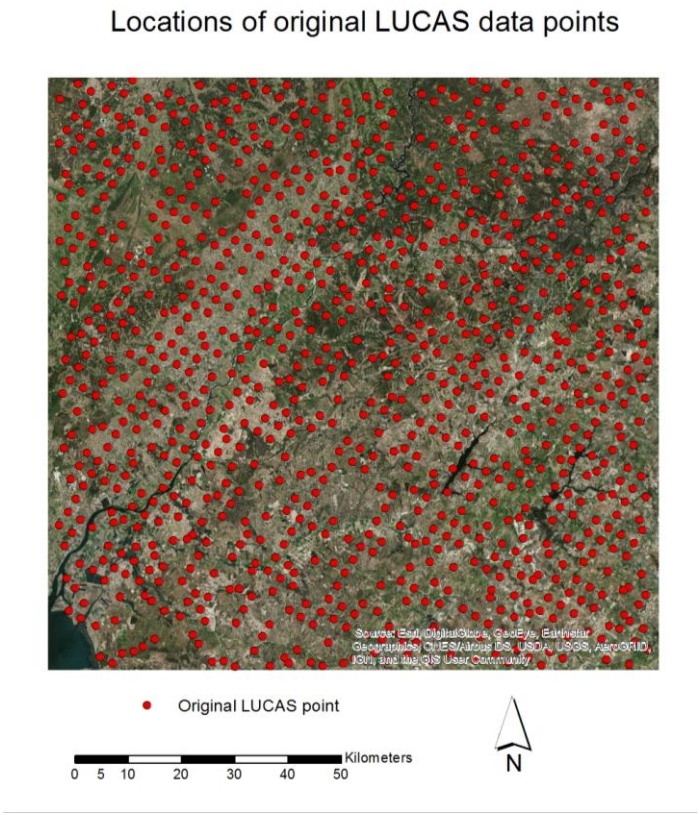

Figure 2. Spatial distribution of original LUCAS samples

The point features were reclassified based on nomenclature used by GeoVille for their HR Land Cover Map for Austria in 2017 (Steidl, 2017) based on a recommendation of Dr. Caetano. The LUCAS technical reference document C3 by Eurostat (EUROSTAT, 2017) was used to correctly reassign every LUCAS sub-class accordingly. The classes composed and their corresponding sample size are visible in **Table 4**. Definitions of the GeoVille nomenclature class criteria were derived from published material and email contact with Ms. Steidl. In the process, two points of the class "Salt marshes" (H21) were excluded, since the GeoVille nomenclature did not include a comparable class. It was concluded that the removal will not negatively impact the training data. This resulted in a final sample size of 962.

GeoVille Category	1- Sealed surfaces	2- Non-vegetated unsealed surfaces	3- Water	4- Woody	5- Herbaceous permanent	6- Herbaceous periodic	Total samples
Corresponding LUCAS Category	**Artificial land**	**Bare land**	**Water**	**Woodland Shrubland Cropland**	**Grassland**	**Cropland**	
Sample size	50	17	14	650	137	94	962

Table 4. Austrian nomenclature and initial sample distribution

Since differentiating permanent from periodic herbaceous is difficult using only spectral values of one month, it was decided to use a binary reclassification scheme for the "Herbaceous periodic" class for the single month maps. Thus, samples of "Herbaceous periodic" were either reassigned to "Non-vegetated unsealed surfaces" or "Herbaceous permanent" (only referred to as "Herbaceous" in single month maps) according to their NDVI value. The threshold for reassignment was set at 0.3, based on recommendations by Dr. Caetano and literature such as Esau et al. (2016). Said paper describes the threshold as significant, stating that surfaces with an NDVI lower than 0.2 normally corresponds to non-vegetated surfaces while green vegetation canopies correspond to an NDVI of >0.3. This process was applied on every single month map to take the Land Cover Change (LCC) caused by seasonal variability into consideration.

From the first experimental classifications with the LUCAS data as training set for the classifier, it became apparent that the data needed to be modified to obtain results with acceptable accuracy. Initial tests on classifying a single month set of imagery achieved an accuracy of 38%. As **Table 4** shows, the distribution of samples on classes is unbalanced with sample sizes ranging from 14 to 650 per class. Unbalanced data means an underrepresentation of an important class in the overall data set (Cieslak and Chawla, 2008). In this sample distribution, "Non-vegetated unsealed surfaces" and "Water" can be described as such.

Unbalanced training data is a common occurrence in data science (Cieslak and Chawla, 2008; Jiménez-Valverde and Lobo, 2006), and it is a phenomenon that frequently occurs when studies use LUCAS data (e.g. Karydas et al., 2015; Mack et al., 2017). To increase classification accuracy, the same approach as in Nitze et al. (2015) and Mack et al. (2017) was taken: Additional samples for the classes two and

three were added to increase information given to the classifier, thus easing the identification of said classes. The approach was to visually identify pure pixels containing a single type of land cover for each class mentioned and label them accordingly. The quantity of added samples was determined by passing the threshold of 50 samples to create more balance and compensate for inaccurate classification attempts during trials. Moreover, initial classification attempts showed the inability of the classifier to distinguish the spectral signatures of water and dense, dark vegetation canopy. Thus 21 samples were added to the class “Woody” to provide additional information. This resulted in a final total sample size of 1056. In addition to this process, some clearly mislabelled sampling points were identified via photointerpretation and moved to reflect their respective class. Not all points were checked. The results of the modifications are in **Figure 3**.

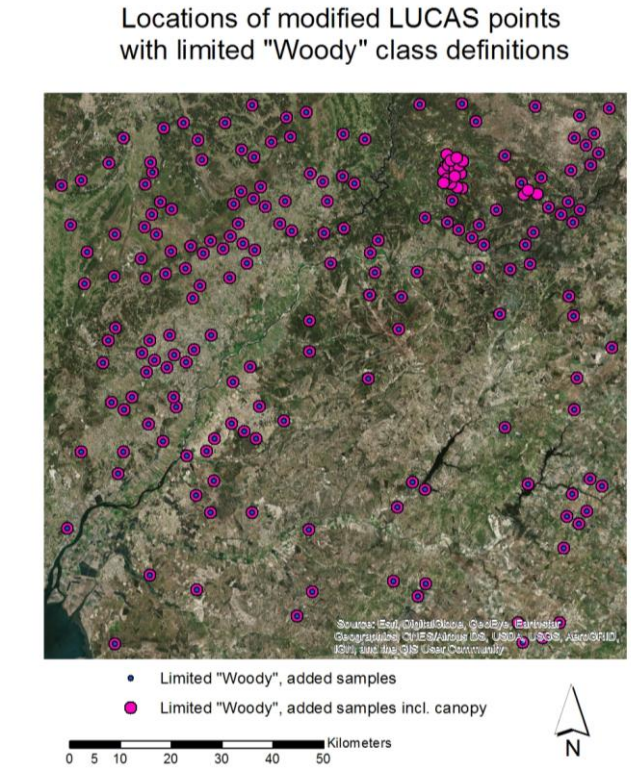

Figure 3. Spatial distribution of LUCAS data sets with a limited “Woody” class

Table 5 shows the final nomenclature used and how it responds to the input LUCAS nomenclature including its subcategories. The final number of samples can be seen in the right column. Added samples are indicated by their label.

ID	Austrian nomenclature	LUCAS main category	LUCAS	Sample sub-category	No. of samples
1	**Sealed surfaces**	Artificial land	A	A11 - Buildings with one to three floors	17
				A21 - Non built-up area features	13
				A22 - Non built-up linear features	20
2	**Non-vegetated unsealed surfaces**	Bareland	F	F10 - Rocks and stones	2
				F20 - Sand	1
				F40 - Other bare soil	14
				Additional samples	34
3	**Water**	Water	G	G11 - Inland fresh water bodies	8
				G21 - Inland fresh running water	6
				Additional samples	39
Excluded	**Snow and ice**	Excluded	Excluded	Excluded	0
4	**Woody**	Woodland	C	C10 - Broadleaved woodland	363
				C22 - Pine dominated coniferous woodland	80
				C32 - Pine dominated mixed woodland	25
				C33 - Other mixed woodland	3
		Shrubland	D	D10 - Shrubland with sparse tree cover	53
				D20 - Shrubland without tree cover	26
		Cropland	B	B71 - Apple fruit	4
				B72 - Pear fruit	3
				B73 - Cherry fruit	1
				B74 - Nuts trees	1
				B75 - Other fruit trees and berries	5
				B76 - Oranges	2
				B81 - Olive groves	65
				B82 - Vineyards	15
				B83 - Nurseries	1
				Bx2 - Permanent crops	3
				Additional samples	21
5	**Herbaceous permanent** Renamed to "Herbaceous" in single month maps	Grassland	E	E10 - Grassland with sparse tree/shrub cover	33
				E20 - Grassland without tree/shrub cover	75
				E30 - Spontaneously re-vegetated surfaces	29
6	**Herbaceous periodic**	Cropland	B	B11 - Cereals	2
				B12 - Durum wheat	1
				B15 - Oats	5
5 or 2	Reclassified into "Herbaceous" or "Non-vegetated unsealed surfaces" depending on NDVI value in single month maps (Threshold: 0.3)			B16 - Maize	33
				B17 - Rice	7
				B18 - Triticale	1
				B19 - Other cereals	1
				B21 - Potatoes	4
				B31 - Sunflower	1
				B42 - Tomatoes	13
				B43 - Other fresh vegetables	3
				B53 - Other leguminous and mixtures for fodder	2
				B54 - Mixed cereals for fodder	1
				B55 - Temporary grasslands	10
				Bx1 - Arable land	10
Excluded	**Reeds**	Excluded	Excluded	Excluded	0
Excluded	**No match**	Excluded	Excluded	H21 - Salt marshes	2

Table 5. Class definitions according to the Austrian nomenclature and LUCAS nomenclature

4. APPROACH, METHODOLOGY AND TOOLS

This section will give an overview over the approach selected as well as the methodology used. **Chapter 4.1** explains the approach taken and gives an overview over the general methodology of the work. It is followed by **Chapter 4.2**, which gives an overview over all tools used in this study. **Chapter 4.3** contains detailed information on the processing of S2 and LUCAS data, followed by the detailed methodology of the analysis conducted in R in **Chapter 4.4**. Finally, the processing of the modified LUCAS data is described in **Chapter 4.5**.

4.1. Approach and General Methodology

The general approach to answering the research questions was kept in close co-operation with the DGT and the co-supervisor of this thesis, Dr. Mário Caetano.
The mapping approach is raster-based with 10m pixel size as the MMU, using categorical values for the land cover classification. For choosing this approach the characteristics of the satellite data, such as its spatial and temporal resolution, as well as the type of thematic information to be extracted have been considered. The characteristics of the geographical area to be mapped, specifically the existing land cover types, and the availability of ancillary data have also been taken into consideration in the general approach, resulting in the nomenclature introduced in **Chapter 3.2.2.** Regarding the classification algorithm, a hard (crisp) classification was used. Unlike with soft (fuzzy) classification, each pixel gets assigned a membership in one definite class (De Matteis et al., 2015). RF was selected, since it is a non-parametric classifier it does not require any assumption about the statistical distribution of the training data while providing good computational efficiency and easy understanding of the classification process (Belgiu and Dra, 2016).

The sample selection for the training phase of the classifier was entirely based on the LUCAS data. Thus, the basic sample size was pre-determined. Additional samples were added to balance underrepresented classes in the training data set as discussed in **Chapter 3.2.2.**
Equalised stratified random points were created in ArcGIS were used as accuracy assessment points of 50 samples per class, following the recommendation of the DGT.

The flowchart showing the methodology to conduct the classification comparison is provided in **Figure 4.** The general flowcharts is composed of the elements listed: unprocessed input data (grey), processes (blue), interstage products (yellow), and final outputs (orange). The grey box indicates the process which had to be repeated ten times, once of each set of single month data.

It consists of six sub-processes necessary to answer the research questions. These sub-processes will be explained in the **Chapter 4.3** and following. All tools used for the analysis are detailed in **Chapter 4.2**.

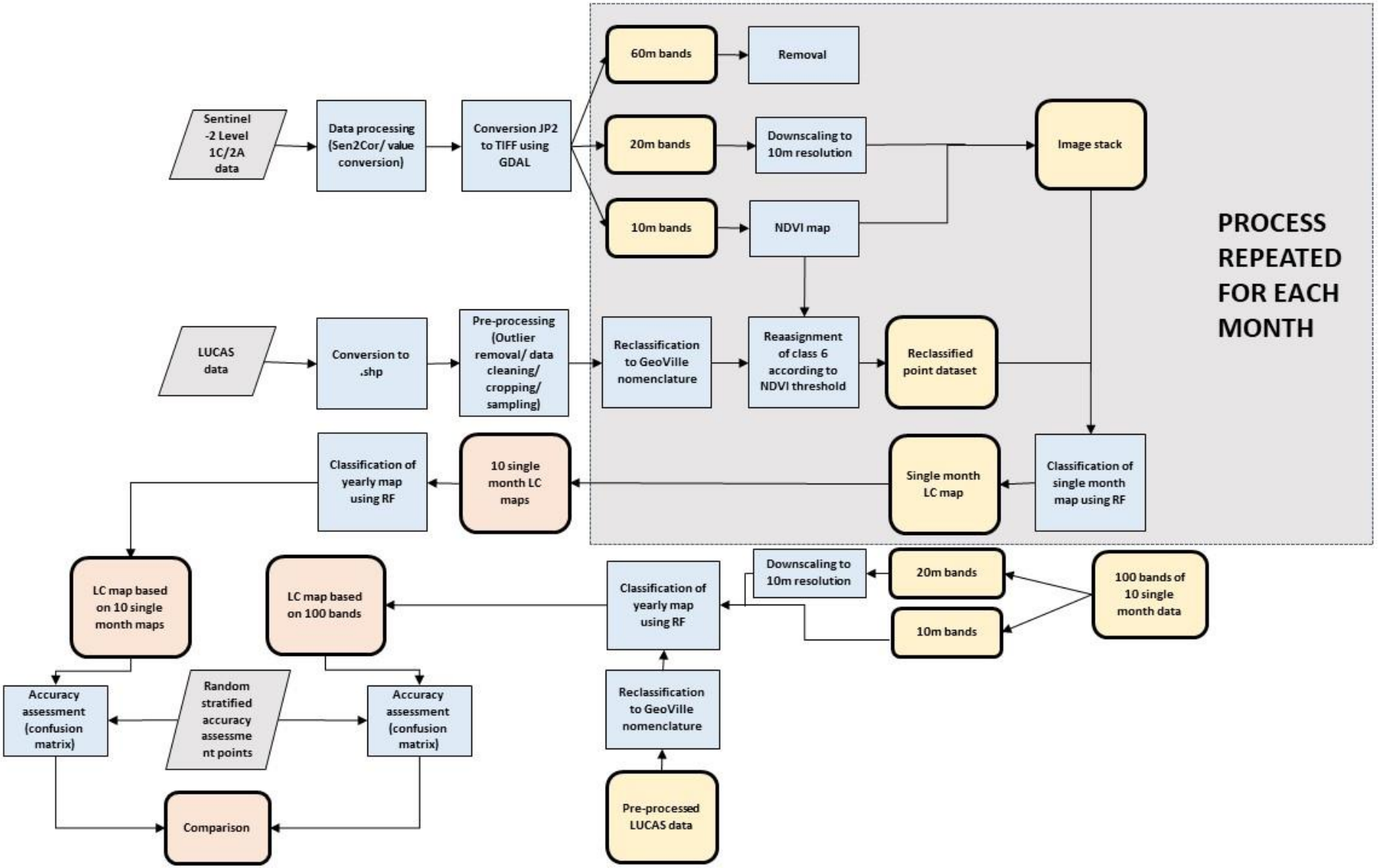

Figure 4. Flowchart showing the methodology of the classification comparison

4.2. Tools

This chapter provides an overview of the tools used in this thesis. **Table 6** shows the tools and respective versions involved in the processing steps. Due to issues with processing capabilities of the author´s computer, the initial computing of the single month maps and all predictions for answering the second research question were done at the DGT using multicore computing. All codes written are in **Appendix C**.

Process	**Tool**	**Version**
General processing	PC	4-core system 300 Gigabyte disc space
Multicore computing	PC	8-core system 1,8 Terabyte disc space
Processing S2 L1C to L2A data	SNAP and Sentinel Toolbox	6.0.0
	Sen2Cor	2.4.0
	Python	2.7.13
Conversion of S2 data from JP2 to TIF	GDAL 202	MSVC 2010 Win64
Processing of LUCAS data	ArcGIS Desktop	10.5.1
Creation of accuracy assessment points		
Pixel redistribution analysis		
Map creation		
Downscaling of 20m resolution bands	R/ RStudio	3.4.2 (64-bit)
Value conversion/NDVI calculation		
Reclassification of nomenclature	Packages	caret 6.0-77 ggplot2 2.2.1 raster 2.6-7 sp 1.2-5 lattice 7.3-47 rgdal 1.2-16 randomForest 4.6-12 e1071 1.6-8 lulcc 1.0.2 snow 0.4-2
Random Forest classifications		
Accuracy assessment		
Creation of graphs	Excel	1712
Class change analysis		

Table 6. Tools and related processes in overview

4.3. Processing of S2 and LUCAS Data

This chapter gives an overview on the processing flows of S2 and LUCAS data used to create the basic interstage products. All future processing is dependent on the execution of those steps.

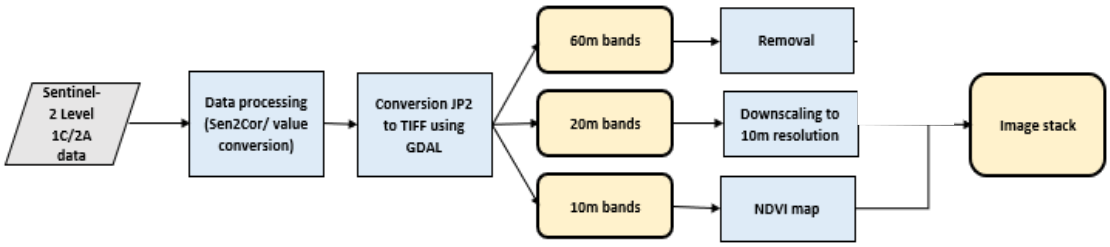

Figure 5. Methodology flowchart of S2 data processing

Figure 5 shows the processing steps of the S2 data to create the image stack used with the classifier. All 130 bands are processed using SNAP´s Sen2Cor toolbox. In this process radiance values are converted into reflectance. This step includes the 30 bands of 60m resolution, since they need to be included in the batch for the processor to function. Additionally, the S2 L2A processing creates L2 ortho-image reflectance products (BOA reflectance) from L1C granules in TOA reflectance. The L2A-processing can be divided into two parts: The Scene Classification provides a pixel classification map (cloud, cloud shadows, vegetation, soils/deserts, water, snow, etc.) and the Atmospheric Correction aims at transforming TOA reflectance into BOA reflectance (**Figure 6**) (ESA, 2017e) .

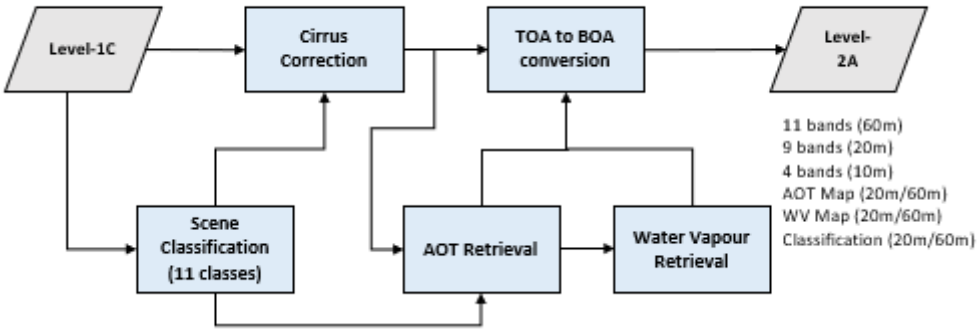

Figure 6. Sen2Cor main processing steps (adapted from Louis *et al.* (2016))

The processing starts with the Cloud Detection/Cirrus Correction and Scene Classification followed by the retrieval of the Aerosol Optical Thickness (AOT) and the Water Vapour content from the L1C product. The final step is conversion from

TOA to BOA (ESA, 2017e). The L2A products are in JP2 format and need to be converted to GeoTIFF for processing in R (2017). For the conversion of all bands, batch conversion was advisable. Thus GDAL (GISInternals, 2017) USGS Raster Conversion Scripts (USGS, 2017) via Windows Command Prompt was used. Subsequently, the bands are divided into monthly batches. The following processing step is the division of the bands according to their spatial resolution in R. The 30 bands of 60m resolution are removed and the 60 bands of 20m resolution are disaggregated to 10m resolution and joined with the initial 40 bands of 10m resolution to a raster stack consisting of 100 bands. Additionally, the NDVI values are extracted from each 10-band single month dataset as a raster using the following equation:

NDVI= (Band 8-Band 4)/(Band 8+Band 4)

This corresponds with the general formula for calculating the NDVI:

$$NDVI = \frac{\rho_{nir} - \rho_{red}}{\rho_{nir} + \rho_{red}}$$ (Matsushita et al.,2007; Schmidt et al., 2014).

The processing of the LUCAS 2015 data is shown in **Figure 7**. After a data type conversion from CSV to shapefile, the data is processed in ArcGIS. This includes removal of unconfident sample points, data cleaning, cropping and additional sampling, as explained in **Chapter 3.2.2**. It is then reclassified in R using the Austrian nomenclature and "Herbaceous periodic" values are reassigned to "Non-vegetated unsealed surfaces" or "Herbaceous permanent" respectively depending on their NDVI value (**Chapter 3.2.2**).

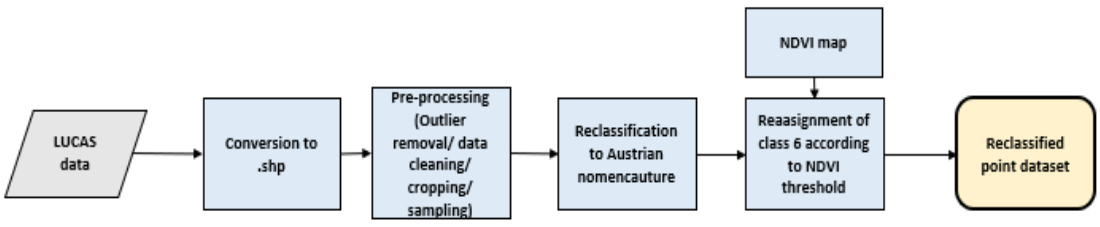

Figure 7. Methodology flowchart of LUCAS data processing

4.4. Analysis in R

All processing and analysis in R is described in this chapter. The ten single month prediction maps and the two land cover classification maps are produced based on the methodology presented here. Moreover, the process used for accuracy assessment is presented.

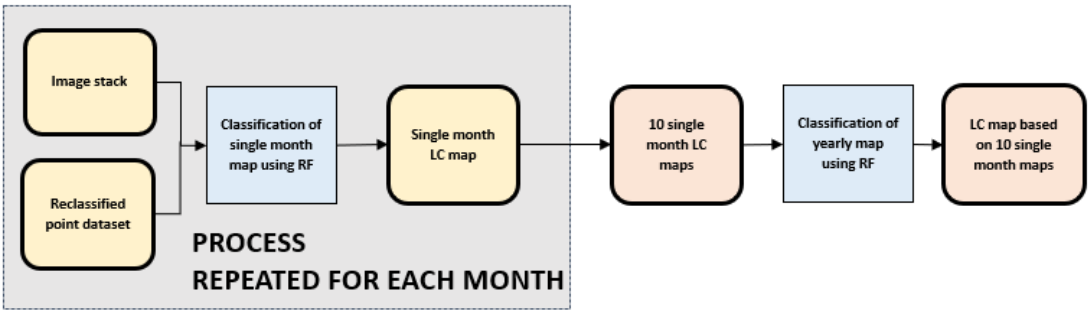

Figure 8. Methodology flowchart of single month map classification to map based on all months

The approach consisted firstly of the production of 10 land cover maps (one for each month) based on the respective image stack and the reclassified point data set. The accuracy of the maps based on single month data was not assessed. This step is followed by the classification of these 10 maps to generate a single map (see **Figure 8**).

The algorithm used is Random Forest in R. For the classification of the single month maps the package "caret" was used. It has a training feature that creates a grid of tuning parameters for a variety of classification and regression routines, then progresses to fit each model, calculates a resampling based performance evaluation (Kuhn, 2017). The model with the best evaluation is then automatically selected for conducting the classification.

For the classification of the map based on the 10 maps the "randomForest" package (Breiman and Cutler, 2015) is used, since there were problems using "caret". The only manually adjusted parameter is the mtry value, which was set to 10. This parameter determines the number of variables that are randomly samples as candidates per split. The mtry value giving the best classification result can be determined using the "train" function of the same package.

Because this process demands relatively high computational power to be finished in a time span of less than two hours, this part of the classification was conducted by Hugo Costa at the DGT using multicore computing. Details can be found in **Table 6** above.

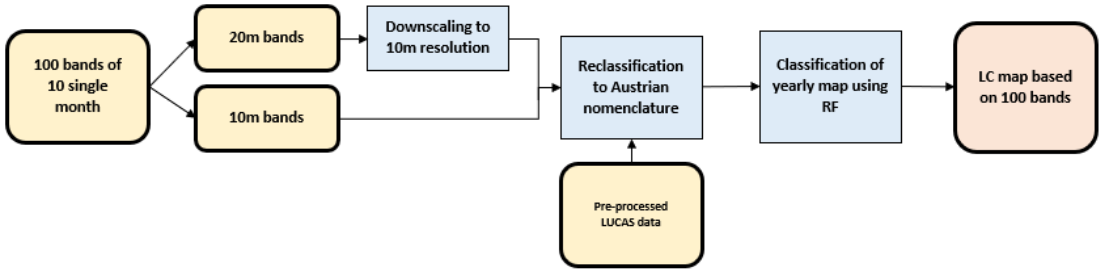

Figure 9. Methodology flowchart of all band-based map classification

The following step is to produce an LCC map based on 100 spectral bands. The L2A data is separated in R and the bands with 20m spatial resolution are downscaled to 10m resolution. All bands are then combined with the pre-processed LUCAS data points and classified using the "caret" package in R. All variables are left at default except that the number of decision trees to grow, "ntree" was set to 500. Like this study, a large amount of scientific papers reviewed for this thesis (e.g. Eisavi et al., 2015; Lawrence and Moran, 2015; Ramoelo et al., 2015; Immitzer et al., 2016; Cánovas-García et al., 2017) set the "ntree" value to 500 for two reasons: Firstly because the errors minimize before the number of classification trees is reached (Lawrence et al., 2006). Secondly its popularity could be explained by the fact that 500 is the default value in the "randomForest" package (Belgiu and Dra, 2016).

The last step of this part of the study was to statistically assess the two main maps. For this purpose, a set of equalized stratified random accuracy assessment points was created in ArcMap based on the CORINE Land Cover Map of 2012. The classes defined in CORINE and represented in the area where redefined according to the classification used in this study. From the areas selected for each class, 50 accuracy assessment points per class were extracted. The quanitiy was based on a recommendation of Hugo Costa. All points where then visually inspected based on orthoimagery of the area taken in August 2017 and reassigned to their respective

classes if the initial classification was inaccurate. This process resulted in an accuracy assessment dataset of 300 samples. These samples are then used for calculating a confusion matrix using the "caret" package (**Figure 10**).

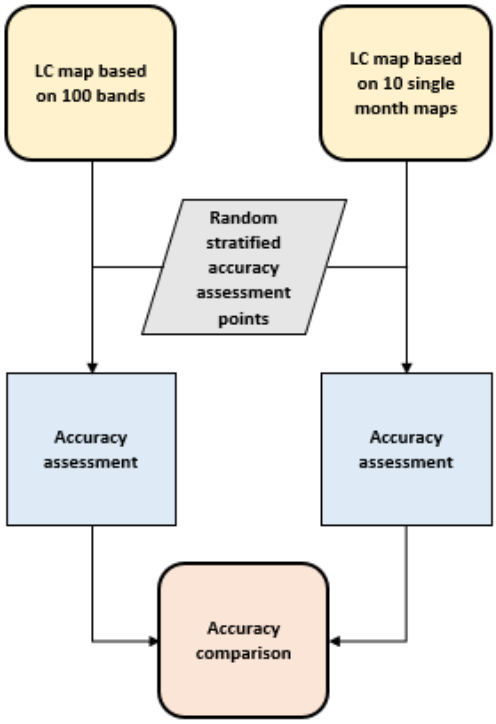

Figure 10. Methodology flowchart of accuracy comparison between classification approaches

4.5. Testing Variations of LUCAS data

The comparison of the classifcation approaches was done using LUCAS data with the modifications explained in **Chapter 3.2.2**. These changes were added sampling to increase sample size in underrepresented classes and to prevent specific misclassifications. It was decided to run three additional classifications to further investigate the accuracy of LUCAS data and to be able to correctly assess its usability.

One additional classification was run with the original data as obtained online. Two were run with adjusted LUCAS data after removing certain sub-classes from the main class "Woody". This step was added after finishing the initial research to test the hypothesis that the classifier should achieve a higher accuracy when LUCAS classes connected to spectral signatures of high ambiguity (e.g. orchards and vineyards) were removed from the analysis. The classes removed were

initially classified as “Woody” though they are sparsely vegetated. This was thought to decrease the overall accuracy of the classification. **Figure 11** shows the approach used which is the same as **Figure 9**, except for the training data.

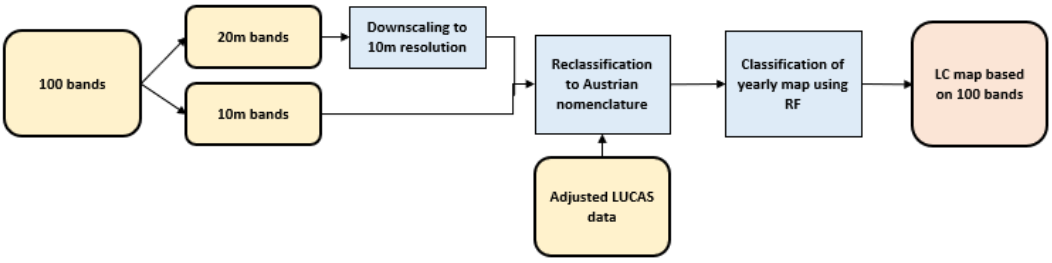

Figure 11. Methodology flowchart of LUCAS variations comparison

The following LUCAS subclasses were removed for the modified variations with a limited class definition of “Woody” (176 samples in total): Shrubland with sparse tree cover, Shrubland without tree cover, Apple fruit, Pear fruit, Cherry fruit, Nuts trees, Other fruit trees and berries, Oranges, Olive groves, Vineyards, Nurseries, and Permanent crops.

For the second variation of the set with a limited definition of classes included in “Woody”, the additional set of manually added points was removed that was initially created to distinguish between the spectral signatures of high density canopy and water. The sample size of the class “Woody” was reduced to 495 and 474 respectively, therefore reducing the final sample sizes to 880 samples and 859 samples respectively.

5. RESULTS AND DISCUSSION

This chapter will present and discuss the results of the analysis. It is divided into five subchapters. Firstly, the NDVI results. **Chapter 5.1** is discussing the results of the redistribution of "Herbaceous periodic" to either the class "Non-vegetated unsealed surfaces" or "Herbaceous" when creating the single month maps. **Chapter 5.2** contains the results of the two approaches covering visual inspection with ortho-imagery, and an analysis of classification differences between the approaches on a pixel level. The following **Chapter 5.3** contains the accuracy assessment and discusses the results of the classifications approaches. **Chapter 5.4** presents and discusses the results obtained when comparing four different variations of the LUCAS dataset as training data for the classifier based on the approach using 100 bands. **Chapter 5** is then concluded with a discussion of the usability of LUCAS data.

5.1. NDVI Results

The reassignment of the samples of "Herbaceous periodic" to "Non-vegetated unsealed surfaces" and "Herbaceous permanent" respectively was determined whether the NDVI value exceeded the threshold of 0.3 in the month currently classified. "Non-vegetated unsealed surfaces" consisted of 51 samples without the reassigned samples, and "Herbaceous (permanent)" consisted of 137 samples. **Figure 12** shows the development of sample sizes of the two classes. Starting with 90 samples and 192 samples respectively in November 2016, there are more samples assigned to "Non-vegetated unsealed surfaces" in the following month. From January to April a sharp decline of samples assigned to "Non-vegetated unsealed surfaces" is visible, which can be considered anti-cyclic regarding the development of the NDVI values normally measured in this vegetation period. A possible explanation for this occurrence is rainfall and warm weather, which could cause spontaneous vegetation of the areas. It needs to be considered though that no data was available for February and March 2017. The NDVI value then increases on average in months known for high crop production (May to July) (Esch et al., 2014). The months leading to autumn are characterised by a decline of sample size classified as "Herbaceous" and thus an increase in sample quanity of the class "Non-vegetated unsealed surfaces", which

corresponds with normal variations of NDVI values caused by cyclic changes in vegetation (Jia et al., 2014).

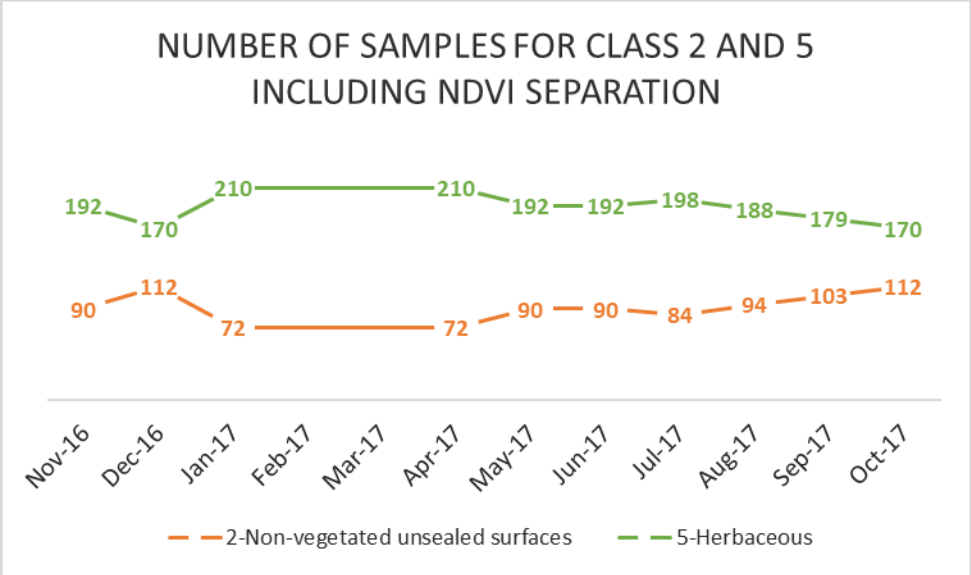

Figure 12. Temporal trajectory of class sizes of "Non-vegetated unsealed surfaces" and "Herbaceous"

These cyclic changes can also be visually identified in the maps based on single months, which are available in **Appendix A- Single Month Maps**.

5.2. Results of the Classifications Approaches

Regarding computational and preparational effort, the approach based on 100 bands was considerably quicker with a total of 5 around hours per map (3 hours data preparation and 2 hours of RF computing time). The approach based on all maps took around 1.5 to 2 hours per map, totalling in around 15h of data preparation and computing.

The author also notes that the classification based on all bands has been conducted twice to test its reproducability. Both times "seeds" were set in R, which allow the user to select the specific RF ensemble again. Since the results of the two classifications only varied minimally, the author will only discuss the approach based on seed number five in the following text. Maps and graphs on seed number 17 can be found in **Appendix B.** This chapter continues with a direct comparison of the two main approaches, the classification based on all single month maps and the classification based on all bands (Seed 5).

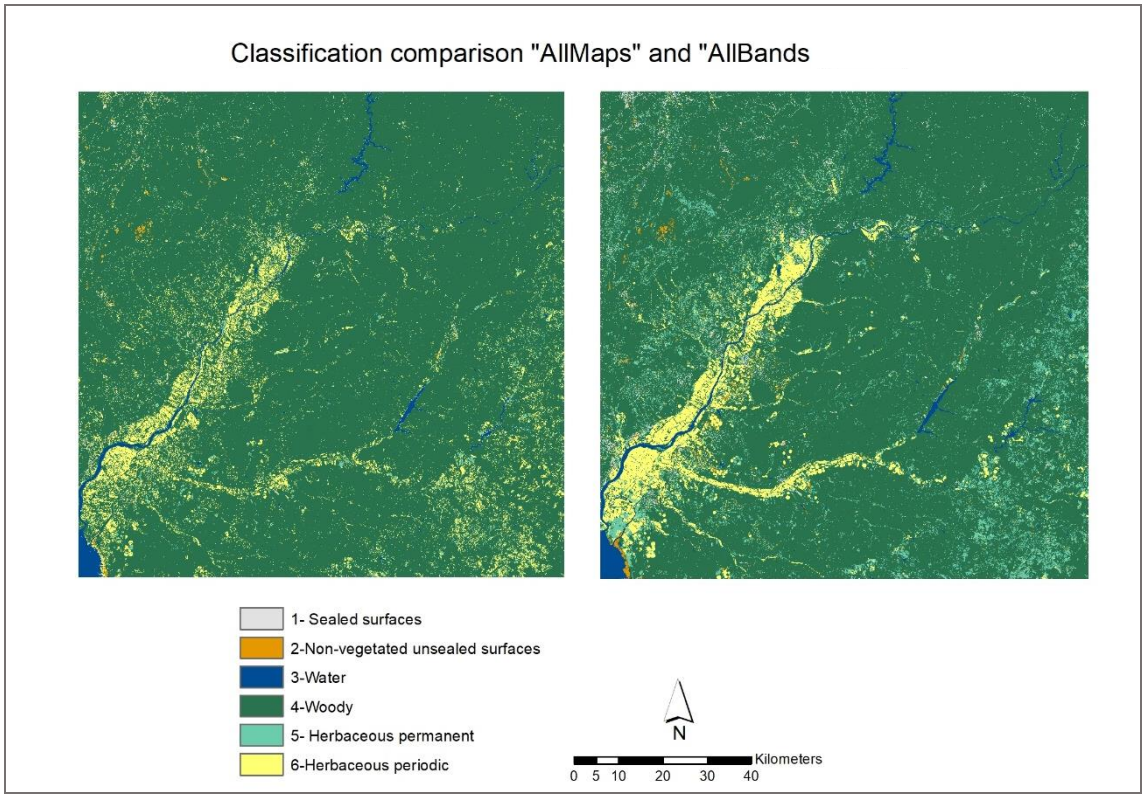

Figure 13. Direct comparison of the classification results

Figure 13 shows a direct comparison of the two maps resulting from the different classification approaches. On the left, the map based on the 10 maps is shown. It represents what the classifier identified as the most probable average land cover of the entire time span covered. On the right, the map based on using all 100 bands within one classification is shown. Compared to land cover types derived from the RS image and the CORINE classification, both classifiers were able to approximately correctly identify waterbodies, agricultural areas, herbaceous areas, and artificial surfaces such as cities. Visual comparison indicates a higher quantity of pixels classified as “Herbaceous periodic” (agriculture) and “Herbaceous permanent” using the approach based on the stack of 100 bands. The area bordering the Tagus river and its river channels shows a higher density of “Herbaceous periodic”, and the North-Eastern and Western part of the study area shows an increased presence of “Herbaceous permanent”. Upon visual inspection, the 100 bands-based approach seem to be more correct, since agricultural lands normally have continuous surfaces and are not mixed with other land cover types within one unit.

Nonetheless, due to the size of the study area of 10 000km^2 in comparison to the pixel size of 100m^2, it is difficult to visually determine detailed changes, thus a

representative region within the study region was identified for closer examination. **Figure 14** shows a region of approximately 20km by 20km in the Tagus region where change can be identified in greater detail.

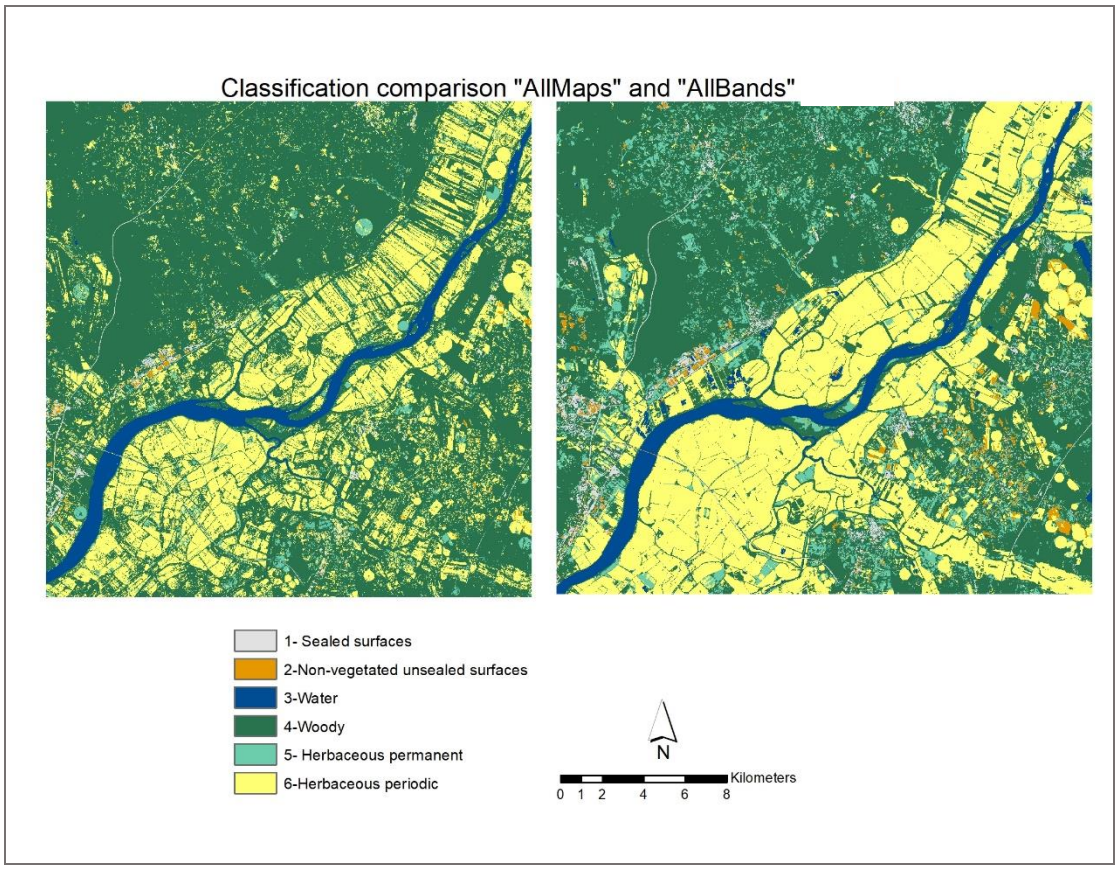

Figure 14. Direct comparison of the classification results enlarged

The assumptions stated above are confirmed upon visual inspection of **Figure 14**. The density of pixels identified as “Herbaceous periodic” is higher using the 100 bands-based approach. Moreover, a larger continuous area is identified to belong to the class. This approach classifies the borders of the agricultural areas crispier and shows a lower ratio of the class “Woody” within these areas. Additionally, the class “Herbaceous permanent” was identified more often using the 100 bands-based approach. To assess which map represents the land cover more accurately, the maps are compared to RS imagery in **Figure 15** and **16**. The 100 bands-based approach represents the agricultural areas and their continuous land cover type of crop more accurately than the map-based approach. A similarity is that both classifiers were able to correctly identify water and artificial surfaces in the area, such as settlements in the North and the street in the West of the study area.

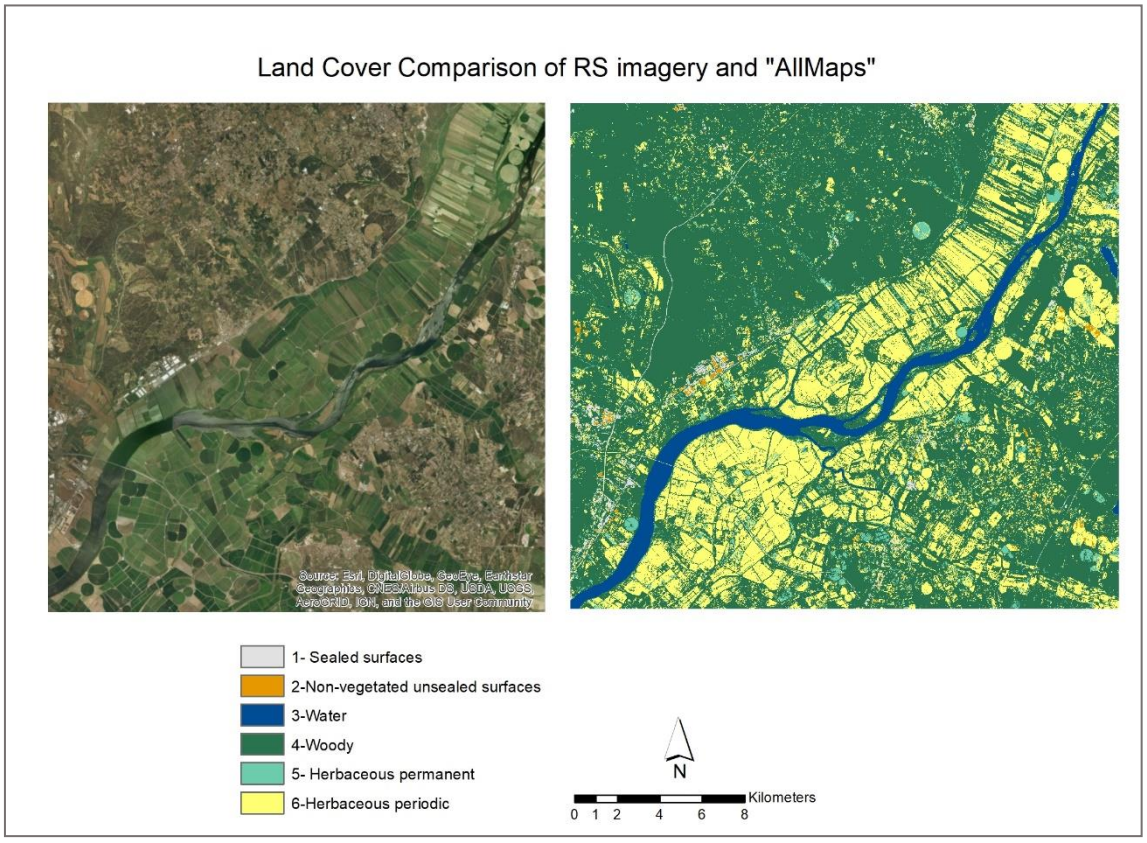

Figure 15. Land Cover Comparison of orthoimage and maps-based approach

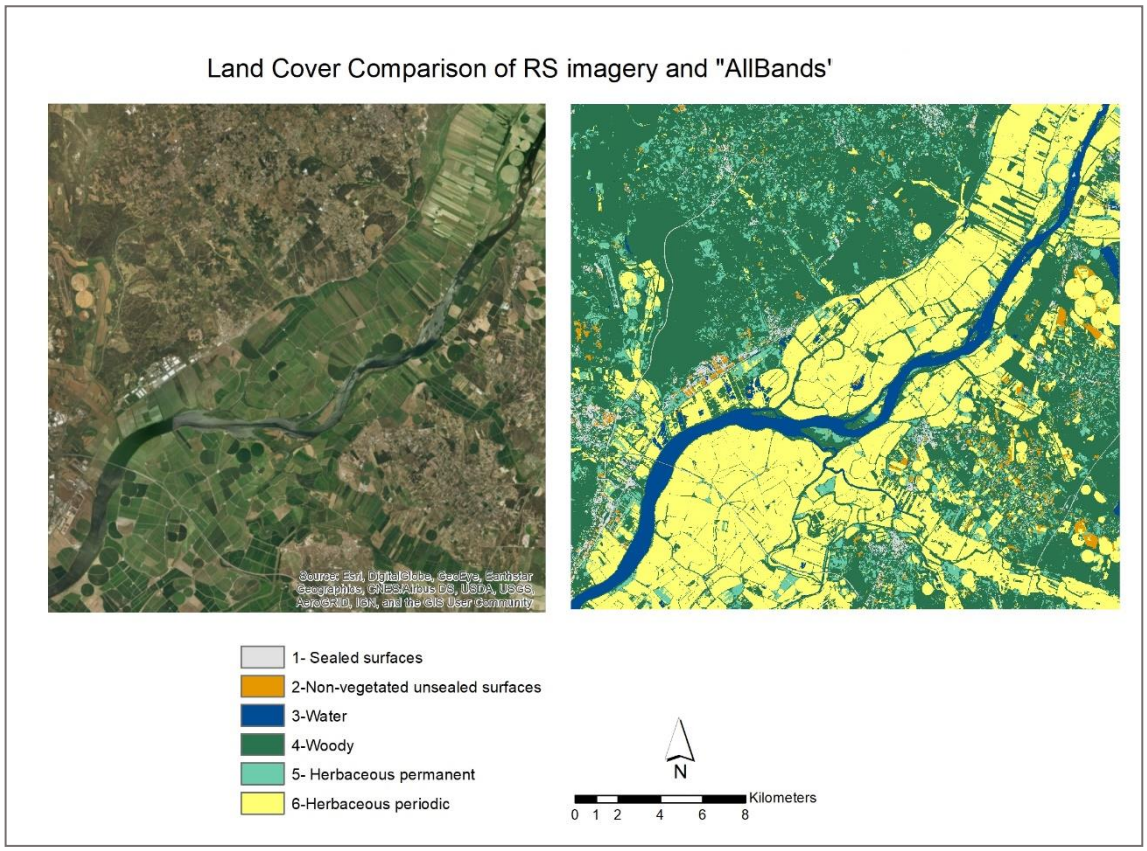

Figure 16. Land Cover Comparison of orthoimage and 100 bands-based approach

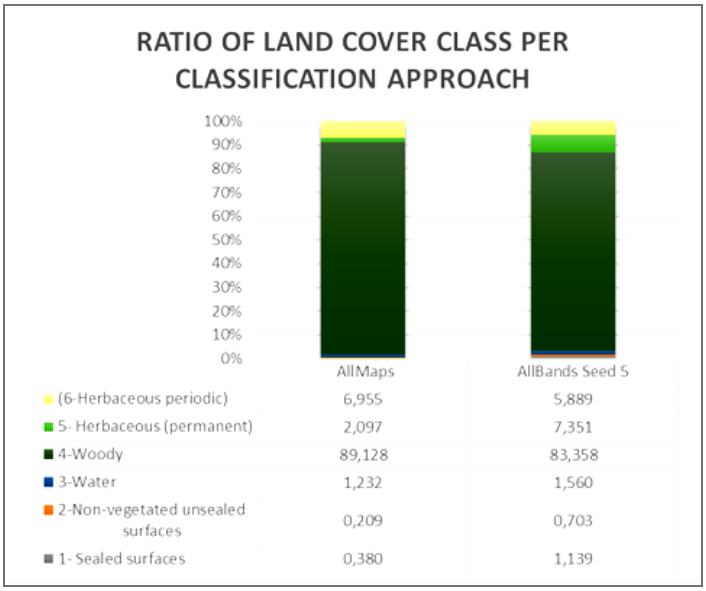

Figure 17. Direct comparison of ratios of land cover classes per classification

The statistics in **Figure 17** confirms the assumptions about the distribution of pixels per class, showing an increase of "Herbaceous periodic" of around 1% and "Herbaceous permanent" of more than 5% in the second classification. The percentage of change of the classes "Water", "Non-vegetated unsealed surfaces" and "Artificial surfaces" vary between 0.3% and 0.8%.

Though singular pixels were assigned to different classes when comparing the classification approaches, the figures above neither identify the locations of the pixels which changed classes, nor the type of change. To contribute this knowledge, a binary change map was created using the Raster Calculator Tool in ArcGIS. **Figure 18** shows the output, identifying location and total percentage of change. The areas of changes are very similar to the ones visually identified, mainly located in the North-East of the study area and in areas with agricultural land use along the river, with a total of 12.98% of pixels assigned to a different class than in the first classification.

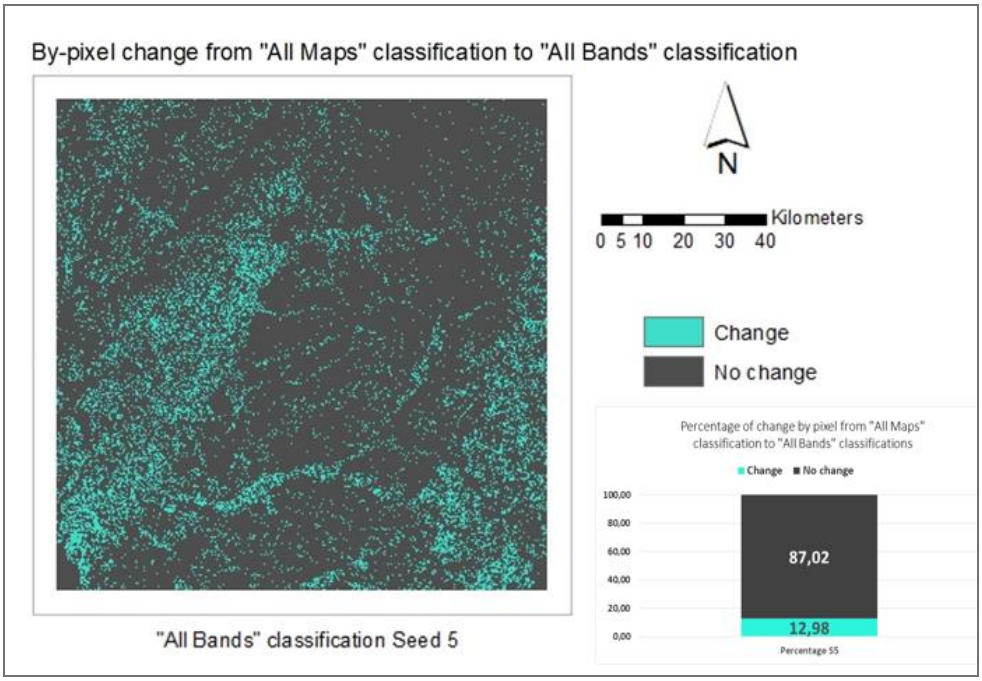

Figure 18. Binary map indicating difference in assigned class per pixel

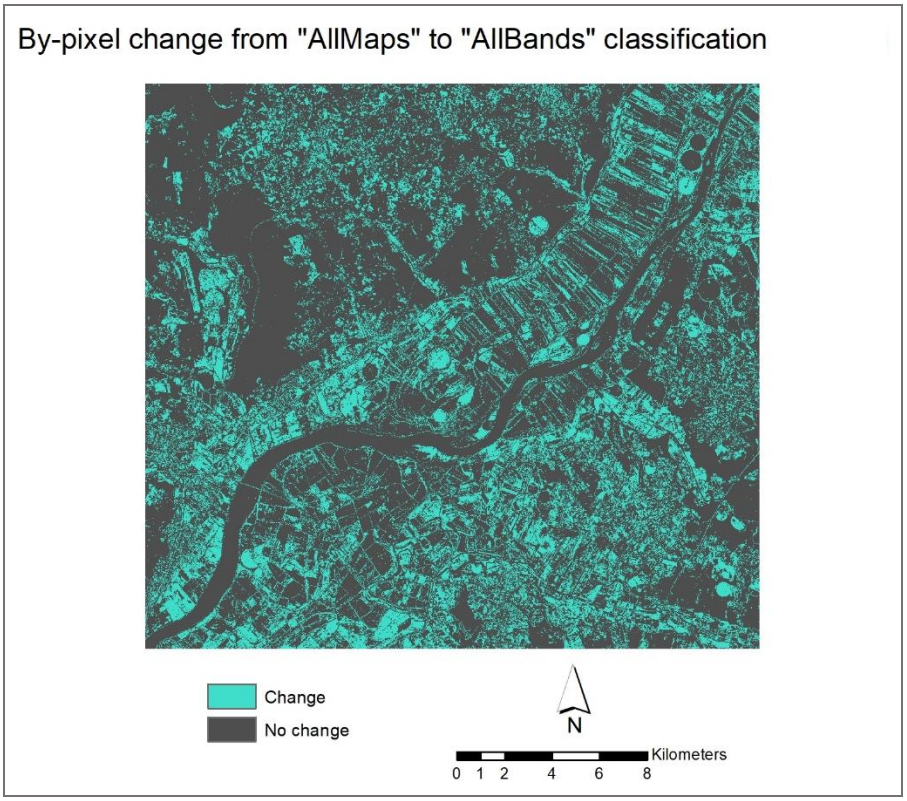

Figure 19. Binary map indicating difference in assigned class per pixel - zoom

Figure 19 confirms that the changes in class-to-class pixel distribution occur between the Classes 4, 5, and 6 ("Woody", "Herbaceous permanent", and "Herbaceous periodic") upon visual inspection. In order to further investigate, the two maps were used to tabulate the area to identify the ratio of class-to-class change between classification approaches. **Table 7** shows which percentage of pixels assigned to each class during the classification based on the single month maps were assigned to the same class during the classification based on all bands, and if this was not the case, which class they got assigned to. It shows a high ratio classes being assigned to the same respective class in both maps for the classes "Sealed surfaces", "Non-vegetated unsealed surfaces", "Water", and "Woody" (91-98%). A significant decrease in overlap is visible in the percentage of pixel re-assignment of "Herbaceous permanent" and "Herbaceous periodic". Only 41.2% and 43.4% respectively were identified to belong to the same class by both approaches. 20% to 27% of the pixels were reassigned to the other two classes belonging to said group. Why these specific classes are so susceptible to misclassification will be discussed in the following chapter.

	AllBands "Sealed surfaces"	**AllBands "Non-vegetated unsealed surfaces"**	**AllBands "Water"**	**AllBands "Woody"**	**AllBands "Herbaceous permanent"**	**AllBands "Herbaceous periodic"**
AllMaps "Sealed surfaces"	90,85	1,42	1,57	4,55	1,42	0,19
AllMaps "Non-vegetated unsealed surfaces"	2,53	93,39	1,25	1,23	1,09	0,52
AllMaps "Water"	0,92	0,44	97,96	0,55	0,1	0,04
AllMaps " Woody"	0,41	0,13	0,17	91,32	5,31	2,67
AllMaps "Herbaceous permanent"	4,22	0,17	4,75	26,54	41,17	23,15
AllMaps "Herbaceous periodic"	4,68	5,49	1,35	19,94	25,14	43,41

Table 7. Percentage of class-to-class redistribution of pixels between classification results

5.3. Accuracy Assessments and Discussion of the Classification Approaches

Upon evaluating the results of the accuracy assessment in **Table 8**, the approach using all bands in one classification process reached significantly better results than the approach based on the single month maps.

	Overall Accuracy	**Kappa**	**Accuracy**	**1-Sealed surfaces**	**2-Non-vegetated unsealed surfaces**	**3-Water**	**4-Woody**	**5-Herbaceous permanent**	**6-Herbaceous periodic**
Classification based on single month maps	0.47	0.36	User Accuracy	0.78	0.56	0.9	0.31	0.47	0.44
			Producer Accuracy	0.14	0.10	0.92	0.96	0.14	0.54
Classification based on 100 bands	0.58	0.49	User Accuracy	0.88	0.75	0.94	0.33	0.37	0.94
			Producer Accuracy	0.42	0.24	0.98	0.94	0.22	0.66

Table 8. Accuracy assessment of the classification approaches

The overall accuracy is 11% higher and the Kappa coefficient increased from 0.36 to 0.49. Both user and producer accuracies for all classes are higher. This is notable, since both approaches are using the same training data and the same classifier. The lowest range with the highest accuracies is of the class “Water”, having 90% and 94% user accuracy and 92% and 94% producer accuracy respectively. This indicates accurate training data for this class and good performance of the classifiers.

The largest difference between user accuracies of the classification approaches are found in “Herbaceous periodic” with a difference of 50%, while the largest difference between producer accuracies are found in “Sealed surfaces”, with a difference of 28%. This class also displayed the largest difference between producer and user accuracy within the same classification approach (14% to 78%), indicating strong inaccuracies within the classification process. All classes but “Water” show a difference in user and producer accuracy of over 5%. This indicates that there is a general issue with the training data, since the large range of values is not connected to one specific class.

The methodology applied in this thesis is not present in current literature thus there were no pre-existing hypothesises available to explain the difference. Nonetheless, a possible explanation for the difference in overall accuracies can be found in the single month classifications. Unlike the map based on the classification of 100 bands, the maps-based prediction is exclusively based on the input of the pre-classified maps for training. Firstly, this is limited information for training compared to the extent of training data available to the classifier in the 100 bands-based approach. Secondly, every misclassification in the single month maps is transferred into the final classification. Due to the limited training data, these misclassifications, if consistent enough throughout the single month maps, can negatively impact the accuracy of the final land cover prediction map.

For testing the accuracy of the classifications obtained, a reference data base consisting of 50 samples per class was used. **Table 9** shows the confusions matrices of the two classification approaches in comparison. In general, it can be stated that the 100 bands-based prediction identified the samples of all accuracy assessment more accurately by assigning them to the same class they have in the reference data. For the class “Sealed surfaces”, the approach correctly predicted 21 of the 50 samples, while the maps-based approach only predicted 7 samples correctly. The same tendency can be observed in most other classes (12 correctly assigned samples compared to 5 for “Non-vegetated unsealed surfaces”, 49 compared to 46 correctly assigned samples for “Water”, 11 compared to 7 correctly assigned samples for “Herbaceous permanent”, and 33 compared to 27 correctly assigned samples for “Herbaceous periodic”). The only exception from this pattern is the class “Woody”, where 48 reference samples were correctly predicted by the prediction based on the single month maps, while 47 reference samples were correctly assigned by the prediction 100 bands-based approach.

	REFERENCE					
PREDICTION OF THE MAPS-BASED APPROACH	1- Sealed surfaces	2-Non-vegetated unsealed surfaces	3- Water	4- Woody	5- Herbaceous permanent	6- Herbaceous periodic
1- Sealed surfaces	7	2	0	0	0	0
2-Non-vegetated unsealed surfaces	4	5	0	0	0	0
3-Water	1	3	46	0	0	0
4-Woody	22	25	0	48	39	22
5- Herbaceous permanent	1	3	2	1	7	1
6-Herbaceous periodic	15	12	2	1	4	27

	REFERENCE					
PREDICTION OF THE 100 BANDS-BASED APPROACH	1- Sealed surfaces	2-Non-vegetated unsealed surfaces	3- Water	4- Woody	5- Herbaceous permanent	6- Herbaceous periodic
1- Sealed surfaces	21	3	0	0	0	0
2-Non-vegetated unsealed surfaces	4	12	0	0	0	0
3-Water	0	3	49	0	0	0
4-Woody	22	22	1	47	38	13
5- Herbaceous permanent	3	9	0	3	11	4
6-Herbaceous periodic	0	1	0	0	1	33

Table 9. Confusion matrices of the classification approaches

The results show high confusion between between the Classes “Woody”, “Herbaceous permanent”, and “Herbaceous periodic” for both approaches. The three classes had no reference samples predicted as the first three classes, but only as each other. Specifically, 39 and 38 reference samples respectively of “Herbaceous permanent” were predicted as “Woody”. Moreover, 22 and 13 reference samples respectively of “Herbaceous periodic” were predicted as “Woody”. Additionally, 22 samples respectively of “Sealed surfaces” and 25 and 22 reference samples respectively of “Non-vegetated unsealed surfaces” were predicted as “Woody”.

This indicates that the way the nomenclature was composed can be a source of error that negatively impacted the classification if it does not distinguish and reflect spectral signatures accordingly. This can have multiple causes. One possible cause is the broad composition of the class “Woody”. It was set to include a wide variety of greenery and forest types to simplify the nomenclature. Broadleaf forests and orchards for example have very different spectral signatures yet were still included into the class “Woody”.

Orchard **Sparse Forest**

Figure 20. Direct comparison of two "Woody" land cover classes showing similar spectral signatures as "Non-vegetated unsealed surfaces" and "Herbaceous permanent"

Additionally, in sparsely vegetated areas the spectral signatures can be similar to other classes such as "Non-vegetated unsealed surfaces" or "Herbaceous permanent" which includes grassland with sparse vegetation. **Figure 20** is also an example for this case. **Figure 21** is an example of differences in spectral signatures in densely vegetated areas, yet both land cover types are assigned to the same class. Since "Woody" is by a large margin the most dominant sample class in this study and is composed of a wide variety of spectral signatures assigned to it, the classifier could assign areas with related land cover types to "Woody". Mack et al. (2017) made a similar observation in their study, where grassland and wetland were misclassified in favour of the dominant class of agricultural land.

Figure 21. Area with naturally grown and artificial canopy

Another issue is closely related to the “Salt and Pepper” effect, which was also present in this study. It refers to the fact that depending on the spatial resolution of the data, several land cover classes can be mixed within the same unit, in the case of this study the 10m by 10m pixel. A common phenomenon in the study area is mixed land cover. **Figure 24** shows an extract of aerial photography where the classes “Herbaceous permanent” (grassland) and “Herbaceous periodic” (crops) are overlapping. The overlapping land cover types are difficult to distinguish for a classifier and can easily lead to misclassification of the affected pixel.

Figure 22. Area with mixed land cover of crops and grassland

Moreover, there was a 2% to 8% misclassification of “Herbaceous periodic” and “Herbaceous permanent” for each of the two classes with each other. The differentiation of grassland (in this study “Herbaceous permanent”) and crops (“Herbaceous periodic”) cannot exclusively be based on the interpretation of spectral characteristics due to variations of the spectral signatures within the vegetation period (Esch et al., 2014). It is also because spectral signatures of different crops and grassland are similar in specific periods of the year. This depends on the type of cultivation, phenology and growth of the crop (Esch et al., 2014). Again, **Figure 22** provides a good example of this in the study area. Yin et al. (2014) also reported difficulties to distinguish grassland and non-irrigated cropland, and provided the hypothesis that the confusion is most likely caused by an intensification of agriculture on croplands that were previously non-irrigated.

The characteristics of crops vary highly depending on the season, the region they are located, the climate, the weather during vegetation periods and the farming type of the farmer (equipment, pesticide use, harvesting time). Since grassland has more

stable, continuous characteristics (**Figure 23**), studies state that crops should be distinguishable from grassland when analysing seasonal development (Esch et al., 2014). According to this statement, the classification approach based the single month maps should reflect seasonal development since the maps it is based on reassigned the samples of the class reflecting agriculture ("Herbaceous periodic") based on their NDVI. Nevertheless 22 samples (of 50 accuracy assessment samples) of "Herbaceous periodic" samples were assigned to "Woody", and 15 "Sealed surfaces" reference samples to "Herbaceous periodic".

Notably the approach using all bands in one classification process scored a higher accuracy in detecting agriculture with 66%. The highest misclassification was again with "Woody" (26%). The outcome of this study thus does not support the claim made in literature, which states that tracking seasonal development leads to higher accuracy in identifying cropland. A possible explanation is that misclassifications of this land cover type conducted in the single month maps were transferred into the final map. This hypothesis will not be assessed yet is a possible topic for future studies.

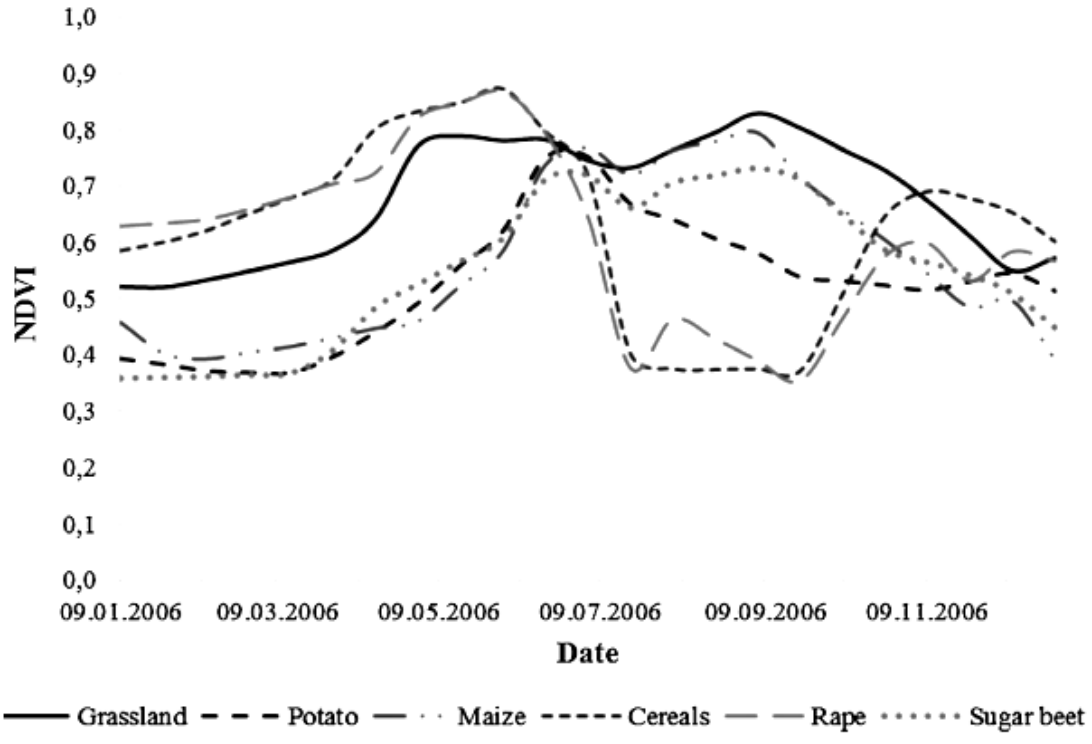

Figure 23. Variation of the NDVI within a vegetation period comparing semi-natural grassland and different crop types (Esch et al., 2014)

Another misclassification to be discussed is the incorrect prediction of “Sealed surfaces” as “Woody” (44%) using both predictions. Karydas et al. (2015) stated a comparable issue when validating a LCC map with LUCAS data, the data all classification in this thesis is based on, when using a single-temporal approach. In the study, their classification showed an almost 14% confusion of “Agricultural land” as “Artificial land” or “Shrubland”. The explanatory hypothesis offered is that mostly roads and small buildings correspond to “Artificial land”. Those features are mostly located inside agricultural areas. Though their study uses and object-based instead of a pixel-based approach, the hypothesis could explain a part of the misclassification due to the aforementioned “Salt and Pepper” effect. Nonetheless, it is questionable if 42% can be entirely explained by this effect.

The class “Non-vegetated unsealed surfaces” also shows confusion with all classes based on incorrect predictions made by the classifiers. A possible explanation is given by Schneider (2012), whose study points out that because of similar spectral values, this class can be confused by the classifier with bare land, uncultivated or fallow agriculture or new construction sites. The highest confusion rate of the “Non-vegetated unsealed surfaces” in both approaches was with the class “Woody” (44% and 50% respectively). **Figure 20** discussed at the beginning of this chapter shows optical similarities between the two land cover types since features such as orchards and vineyards with a high ratio of bare land and comparably little greenery are included in “Woody”.

5.4. Results and Discussion of the LUCAS Training Data Comparison

After discussion the results obtained by using the two different classification approaches, this chapter will show the results of the four variations in LUCAS training data and discuss them.

Since most classes in the accuracy assessment of the classification approaches have the highest misclassification rate with the class “Woody”, it is suggested to consider the arguments made at the beginning of the previous chapter. It was stated

that “Woody” is not only the most dominant class with more than 500 samples more than the second dominant class (“Herbaceous permanent”) and 600 more than the smallest class (“Sealed surfaces”), but it also entails a range of spectral values similar to those of other classes. This combination is likely to be the main cause of the high percentage of class-based and thus overall misclassifications. This hypothesis is tested in this chapter by running additional classifications and assessing their accuracy.

For the first attempt, a classification was run using the original, unmodified LUCAS data and an extensive definition of “Woody” (including shrubland and agricultural woods). The second set used is the one the classification comparison is based on. There, the classifier was trained with LUCAS with added samples to balance the sample sizes per class and counterbalance issues found in trial predictions. Moreover, the extensive class definition of “Woody” was used. In the last two variations, a variety of LUCAS subclasses intially assinged to “Woody” were removed (176 samples in total): Shrubland with sparse tree cover, Shrubland without tree cover, Apple fruit, Pear fruit, Cherry fruit, Nuts trees, Other fruit trees and berries, Oranges, Olive groves, Vineyards, Nurseries, and Permanent crops. One variations only this composition, while for the second attempt with the limited class definition of “Woody” an additional set of manually added points was removed. The decision to add these points were based on a particular misclassification between two classes at the initial stages of the study was the confusion of water and dark forest canopy by the classifier. This error was compensated by adding 21 samples of dark forest canopy to give more information about the exact spectral signature to the classifier.
The sample sizes of the class “Woody” was thus reduced to 495 and 474 respectively, therefore reducing the final sample sizes to 880 samples and 859 samples respectively.

When running the RF classifier based on all bands on the LUCAS data variations as training set, the resulting land cover classification showed significant differences in the ratios of land cover type. **Figure 24** shows the percentage of land cover class per classification. There is no significant deviation from the results produced with the regular LUCAS in the classes “Sealed Surfaces”, “Non-vegetated unsealed surfaces”, “Water”, and “Herbaceous periodic”. Analysing the class size of “Woody” and

“Herbaceous permanent”, several things can be observed: Firstly, there is a difference of maximum 2% between the original LUCAS data set and the set with added samples and extensive class definition of “Woody”. The same can be observed when comparing the two training data sets using a limited class definition of “Woody”. Secondly, when comparing the four sets, it can be concluded that the classifier assigned up to 9% less pixels to “Woody” when using training sets based on a limited class definition of “Woody” in comparison to classification based on the extensive class definition. Instead, up to 8% more pixels were assigned to “Herbaceous permanent”.

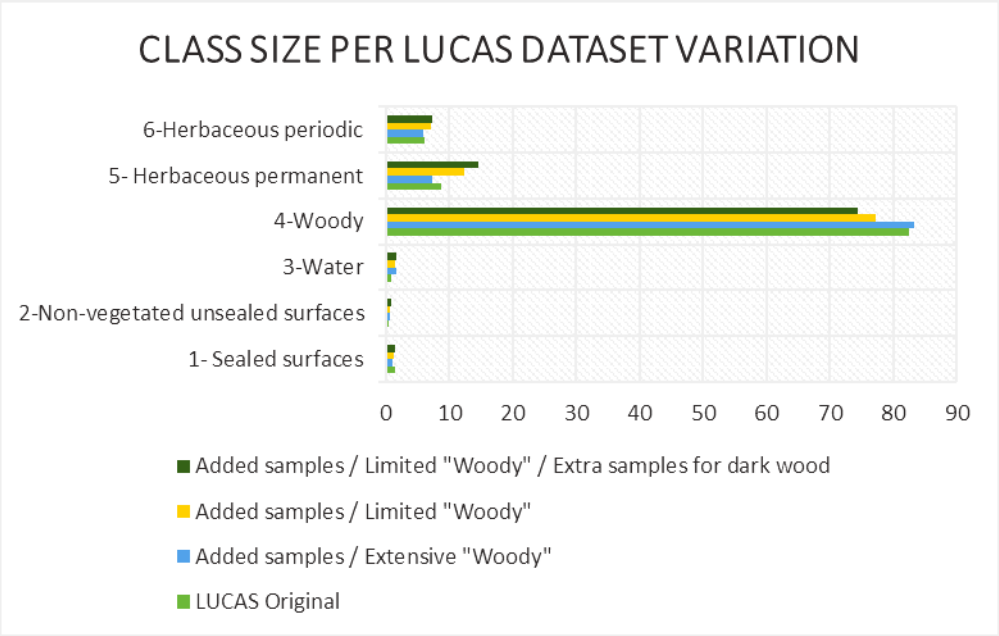

Figure 24. Percentage of land cover type classified with the variations of LUCAS for training

Visual inspection of the maps (**Figure 25**) confirms this outcome, displaying large areas classified as “Herbaceous permanent” in the South-East of the study region as well as the entire region west of the river. Similar to the classification using all bands, it identified a large area of “Herbaceous permanent” close to the river mouth. Moreover, it also shows rather continuous regions identified as “Herbaceous periodic”, which is an accurate representation of the real land cover. Notably, the classifier using the original LUCAS dataset as training data was unable to identify the water feature in the South-Western corner of the study area. This implicated the need for the additional samples to increase the sample size of the class, an approach that created better results, as visible in the other three classifications.

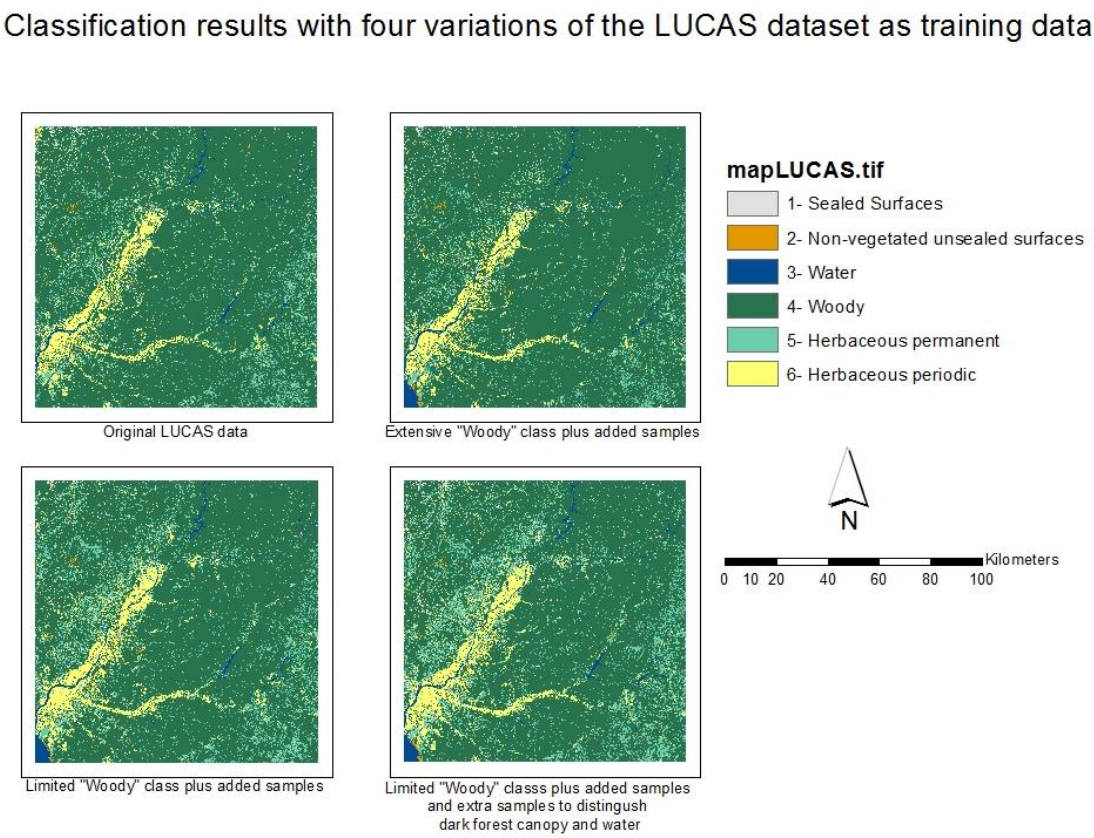

Figure 25. Comparison of map resulting from classifications based on different variations of LUCAS based on training data

As indicated above, the result based on unaltered LUCAS data appeared to have the lowest accuracy. **Table 10** confirms this impression. The predictions based on the original LUCAS data achieved the lowest overall accuracy of 52% of all approaches and a kappa value of 0.42. This is 10% less than the highest overall accuracy achieved by the training set composed of adjusted LUCAS data (including dark canopy samples) and a limited "Woody" class definition. This data set also has the highest kappa value of 0.54.

While the unmodified LUCAS data as training data achieved the lowest accuracy, the training set based on modified LUCAS data and an extensive class definition of "Woody" reached a 58% overall accuracy and a kappa coefficient value of 0.49. This can be explained by the samples added to support underrepresented classes and balance the training data set. An improve of 3% in overall accuracy from this classification to the modified data set using a limited class definition of "Woody" takes place. This result confirms the hypothesis stated in the previous chapter that the land cover types summarized in "Woody" are too broad and possibly confusion for the classifier.

The differences between the two classification approaches based on modified LUCAS data and a limited class definition of “Woody” showed a difference of 0.01 per metric, reaching higher accuracy when the extra samples to distinguish dark forest canopy from water are included. This indicates that even though “Woody” is the largest and most dominant class in the training set, certain spectral signatures are still not represented enough to provide sufficient information to the classifier to distinguish them from similar ones.

Dataset	**Overall Accuracy**	**Kappa**
Original LUCAS data	0.52	0.42
Extensive "Woody" class definition Additional samples	0.58	0.49
Limited "Woody" class definition Additional samples	0.61	0.53
Limited "Woody" Additional samples With samples for dark canopy/water differentiation	0.62	0.54

Table 10. Overall Accuracy and Kappa coefficient of the LUCAS training data variations

The user and producer accuracies of the training data variations indicate the same. In **Table 11**, the producer accuracy of “Water” based on the original LUCAS data shows a significant drop in accuracy of more than 20% compared to all other accuracies of the class. Again, the third and fourth data set achieved higher accuracies than the first two training sets, with the original LUCAS data set having lower accuracies in most classes. The accuracy assessment shows similar patterns as the one conducted on the approach based on all bands in the previous chapter: “Water” has consistently the highest user and producer accuracies of all classes, with exception of the case stated above. The ratio between user and producer accuracy per class and prediction is relatively constant throughout the results (e.g. the difference between user and producer accuracy of “Herbaceous periodic” is in every prediction is 0.25 +/- 0.05 or 0.5 +/- 0.02 for “Non-vegetated unsealed surfaces”). The accuracies of the predictions are overall still low, but show a general increase from the first to the fourth data set used.

Dataset	Accuracy	1-Sealed surfaces	2-Non-vegetated unsealed surfaces	3-Water	4-Woody	5-Herbaceous permanent	6-Herbaceous periodic
Original LUCAS data	User Accuracy	0.79	0.64	0.97	0.31	0.28	0.89
	Producer Accuracy	0.46	0.14	0.72	0.92	0.22	0.64
Extensive "Woody" and	User Accuracy	0.86	0.75	0.94	0.33	0.37	0.94
Added samples	Producer Accuracy	0.42	0.24	0.98	0.94	0.22	0.66
Limited "Woody and"	User Accuracy	0.92	0.8	0.96	0.36	0.38	0.87
Added samples	Producer Accuracy	0.48	0.32	0.98	0.90	0.30	0.66
Limited "Woody", Added samples and	User Accuracy	0.89	0.78	0.92	0.37	0.42	0.92
Samples for dark canopy	Producer Accuracy	0.50	0.28	0.98	0.90	0.36	0.68

Table 11. User and producer accuracy of the LUCAS training data variations

The analysis of the confusion matrices derived from the four different predictions (**Table 12**) confirm the statements made above. The prediction based on the original LUCAS data shows that 22% of reference samples of “Water” were predicted as “Woody”, 2% as “Sealed surfaces”, and 4% as “Herbaceous permanent”. After having the samples to distinguish dark forest canopy from water, the following three predictions correctly predict 98% of “Water” samples and misclassify only one sample as “Woody”. Thus, the hypothesis of underrepresentation of certain spectral values even in large sample sizes of LUCAS seems plausible. Again, the confusion matrices show similar patterns to the matrices of the classification approaches. There is a particular confusion among the classes “Woody”, “Herbaceous permanent”, and “Herbaceous periodic”. Moreover, “Sealed surfaces” and “Non-vegetated unsealed surfaces” reference samples were wrongly predicted as almost all other classes again. All these confusions decrease from the prediction made with the original dataset to the one with the heaviest modifications. Reasons for this were discussed in the previous chapter.

	REFERENCE						
PREDICTION USING ORIGINAL LUCAS DATA		1- Sealed surfaces	2-Non-vegetated unsealed surfaces	3- Water	4-Woody	5- Herbaceous permanent	6- Herbaceous periodic
	1- Sealed surfaces	23	3	1	0	1	1
	2-Non-vegetated unsealed surfaces	4	7	0	0	0	0
	3-Water	0	1	36	0	0	0
	4-Woody	18	24	11	46	37	12
	5- Herbaceous permanent	5	12	2	4	11	5
	6-Herbaceous periodic	0	3	0	0	1	32

	REFERENCE						
PREDICTION USING EXTENSIVE "WOODY"		1- Sealed surfaces	2-Non-vegetated unsealed surfaces	3-Water	4- Woody	5- Herbaceous permanent	6- Herbaceous periodic
	1- Sealed surfaces	21	3	0	0	0	0
	2-Non-vegetated unsealed surfaces	4	12	0	0	0	0
	3-Water	0	3	49	0	0	0
	4-Woody	22	22	1	47	38	13
	5- Herbaceous permanent	3	9	0	3	11	4
	6-Herbaceous periodic	0	1	0	0	1	33

	REFERENCE						
PREDICTION USING LIMITED "WOODY"		1- Sealed surfaces	2-Non-vegetated unsealed surfaces	3-Water	4-Woody	5- Herbaceous permanent	6- Herbaceous periodic
	1- Sealed surfaces	24	2	0	0	0	0
	2-Non-vegetated unsealed surfaces	4	16	0	0	0	0
	3-Water	0	2	49	0	0	0
	4-Woody	19	19	1	45	32	10
	5- Herbaceous permanent	2	10	0	5	15	7
	6-Herbaceous periodic	1	1	0	0	3	33

	REFERENCE						
PREDICTION USING LIMITED "WOODY" AND EXTRA DARK CANOPY SAMPLES		1- Sealed surfaces	2-Non-vegetated unsealed surfaces	3-Water	4-Woody	5- Herbaceous permanent	6- Herbaceous periodic
	1- Sealed surfaces	25	3	0	0	0	0
	2-Non-vegetated unsealed surfaces	4	14	0	0	0	0
	3-Water	0	3	49	0	0	1
	4-Woody	18	20	1	45	30	7
	5- Herbaceous permanent	3	9	0	5	18	8
	6-Herbaceous periodic	0	1	0	0	2	34

Table 12. Confusion matrices of the LUCAS training data variations

Table 13 is showing how the reference database was redistributed to the classes in each classification based on a different variation of the LUCAS data for training. While the class size of the reference database was 50 per class, all four approaches display a similar tendency of having samples of different classes assigned to “Woody”. This class size ranges from 121 samples (using the training data with a limited “Woody” class and added samples) to 148 (using the original LUCAS data). In all four classification approaches, the class of “Herbaceous periodic” contained 35 to 38 samples. This indicates a misclassification of 15-12 samples, yet also shows that variations in the training data had little effect on the classification outcome. A similar result was obtained with the class “Sealed surfaces”, displaying a range of 24 to 29 samples in this class.

“Herbaceous permanent”, whose class size ranged from 30-43 samples, displayed a range of 13. The smallest sample size was achieved when using added samples and an extensive class definition of “Woody”. The class “Water” achieved on average the amount of samples closest to the initial reference data base class size. While the training data sets with added samples resulted in a range of sample sizes of 51 to 53, the classification based on the original LUCAS data showed a strong decrease in class size by 13 samples. This can be caused by the confusion of water and dark forest canopy described above.

Classification	**1-Sealed surfaces**	**2-Non-vegetated unsealed surfaces**	**3-Water**	**4-Woody**	**5-Herbaceous permanent**	**6-Herbaceous periodic**
Reference Database	50	50	50	50	50	50
Original LUCAS data	29	11	37	148	39	36
Added samples Extensive "Woody"	24	16	52	143	30	35
Added samples Limited "Woody"	28	18	53	121	43	37
Added samples Limited "Woody" Extra samples for dark wood	26	20	51	126	39	38

Table 13. Assigned class of accuracy assessment points per training data variation

To further assess the impact of removing samples from the class “Woody” which correspond to shrubland and agricultural woody plants, it is analyzed to which class the removed samples were assigned to in the predictions (**Table 14**). It is shown

that in over 70% of the cases, the samples were again assigned to “Woody”. The class to which the largest percentage of samples was changing classification to is “Herbaceous permanent”. Around 14% and 22% respectively got identified as this class after being removed. This shows that by removing samples from the class “Woody” and limiting the land cover types included in this class, the classifier includes less spectral signatures in it. No sample was assigned to “Non-vegetated unsealed surfaces”, only about 0.5-1% got identified as “Sealed surfaces” or “Water”. Around 6% of the samples were classified as “Herbaceous periodic” using both training sets, which can be explained by similar spectral signatures.

Added samples	**1- Sealed surfaces**	**2- Non-vegetated unsealed surfaces**	**3- Water**	**4- Woody**	**5- Herbaceous permanent**	**6- Herbaceous periodic**	**Total samples**
Sample size	1	0	2	155	27	12	197
In percentage	0,51%	0%	1,02%	78,68%	13.71%	6,09%	100%
Added samples, Extra samples for dark wood	**1- Sealed surfaces**	**2- Non-vegetated unsealed surfaces**	**3- Water**	**4- Woody**	**5- Herbaceous permanent**	**6- Herbaceous periodic**	**Total samples**
Sample size	1	0	0	126	38	11	176
In percentage	0,57%	0%	0%	71,59%	21,59%	6,25%	100%

Table 14. Classes assigned to removed “Woody” samples in the predictions

5.5. Discussion of the Usability of LUCAS Data

When paying attention to the metadata of the LUCAS points, the issue of remote assessment also discussed by Karydas et al. (2015) becomes apparent. **Attribute 2.15** in EUROSTAT (2016) describes the distance in meters between the point planned to survey and the reached point when conducting the survey. **Figure 26** shows a histogram with binned values, excluding the 94 supervised samples added through photointerpretation.

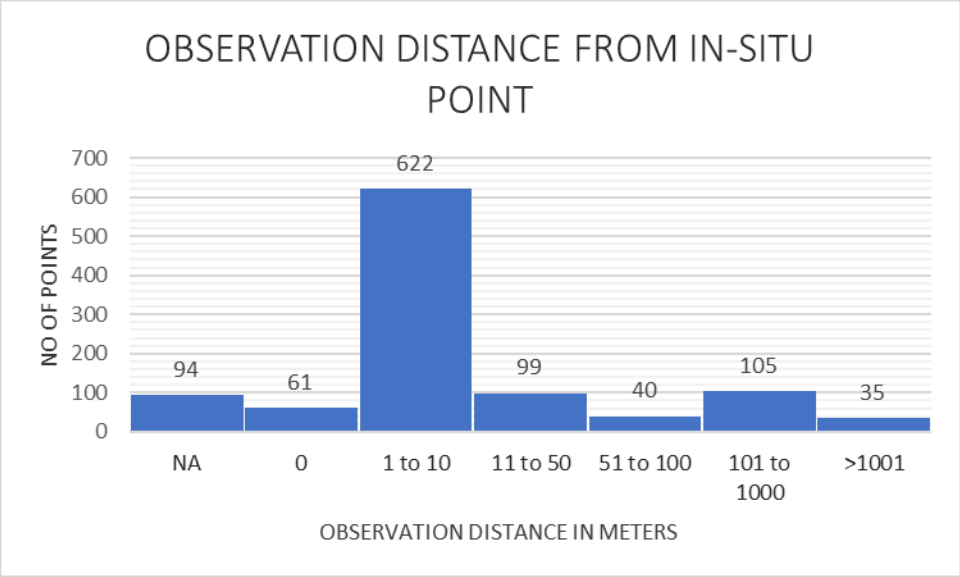

Figure 26. Distance between in-situ point of LUCAS data and observation point

The histogram shows that 71% of initial 962 LUCAS samples were classified within a 0m to 10m distance to the in-situ point. The descriptive statistics show a range of 0m to 4124m, the latter being the largest sampling distance in the batch. 14.45% were sampled between 11m and 100m distance, and the remaining 14.55% were sampled between 1001m and 4024m away from the theoretical point. The average sample distance for the points used is 100m.

With about 30% of the data being classified more than 10m away from the planned sampling point, a high impact on results is probable since all bands used for the project were downscaled to a 10m resolution. Full descriptive statistics for the variable are in the **Appendix B – Additional Maps and Statistics**.

Similar to this study, Karydas et al. (2015) conducted extensive validation of the LUCAS points based on statistics and photo inspections. The study identifies several additional possible sources of error and uncertainty:

According to the LUCAS survey protocol provided by EUROSTAT, if a crop cannot be identified the surveyor should record it either as “Bare land” if less than 50% is covered in weed or as “Spontaneous re-vegetated surfaces” which corresponds to “Herbaceous permanent” in the nomenclature of this thesis. This protocol can cause agricultural land to be misclassified by the field surveyors and thus be mislabelled in the training database of this study, affecting the final accuracy assessment.

Another possible cause of uncertainty raised by this study and Karydas et al. (2015) is that part of the LUCAS points were classified inaccurately by the surveyor. This issue can be related to the issue of remote assessment and photointerpretation discussed earlier in this chapter. Upon interpreting satellite imagery of the area within the initial classification process, it became apparent that some points were not assigned to the correct class. For example, four of the fourteen samples for the class "Water" provided by LUCAS were not located in waterbodies (**Figure 27**).

Figure 27. Original LUCAS sample locations for the class "Water

This does not affect studies using big sample sizes significantly, yet in the case of this study and its sample sizes used, it is expected to lower the final accuracy.

The relatively small sample size of multiple classes leads to another uncertainty: The newest version of LUCSA data available is from 2015, while the classification is based on late 2016 until late 2017 imagery. The class assigned to the sample point, though correctly assigned by the field surveyor, may not be accurate anymore. Since land cover normally does not change rapidly, only a small amount of samples would be affected. Yet when considering the total training data set size per class is only 50 to 60 points for three of the six classes, there is a measurable effect.
Due to the possible causes of uncertainties discussed above Karydas et al. (2015) labelled 23.7% of the points used for their study as impossible to be assessed and removed them.

Though many disadvantages of LUCAS data are discussed here, it is one of the largest OA datasets for LULC information. The data does have good potential and can

achieve high accuracies, as studies using LUCAS data on soil erosion modelling (Panagos et al., 2014), soil pH mapping (Gardi and Yigini, 2012), land cover differentiation (Esch et al., 2014) and LULC mapping (Mack et al., 2017) show. To achieve high accuracies, LUCAS data should be combined with ancillary data and supported by additional sampling.

6. CONCLUSIONS

The study conducted allowed to answer both research questions. Regarding the first question of assessing and comparing the two multi-temporal, multi-spectral classification approaches with RF, the following can the concluded: The results of this study show that the approach based on the simultaneous classification of 100 bands generated a map 11% higher in accuracy than the approach based on the classification of 10 maps based on single month data, which were subsequently used as training data for the RF classifier to make a final prediction. Moreover, the approach was considerably quicker with a total of 5 around hours per map (3 hours data preparation and 2 hours of RF computing time). The approach based on all maps took around 1.5 to 2 hours per map, totalling in around 15h of data preparation and computing. Thus, of the two approaches tested, the land cover prediction based on a stack of bands performed better and required less time and should thus be further explored as an alternative for multi-temporal, multi-spectral classification.

Since the predictions are based on the same training data, the lower accuracy should be caused by the methods used. Two possible sources of error in the methodology of the classification based on the single month maps are identified: Firstly, the limited training data of 10 maps and secondly the possible transfer of classification errors from the single month maps to the final map. Moreover, the outcome of this study thus does not support the claim made in literature, which is that tracking seasonal development leads to higher accuracy in identifying cropland. On the contrary, the classifier which is not considering seasonal development of crops by including the NDVI achieved a higher accuracy in correctly assigning this land cover type.

Additionally, this study indicates that the composition of the nomenclature used had an impact on the classification accuracy. The accuracy assessment and discussion indicated that the broad classification of the class “Woody” can be identified as a cause of the low accuracy results. It was set to include a wide variety of greenery and forest types to simplify the nomenclature. Since “Woody” is by a large margin the most dominant sample class in this study and is composed of a wide variety of spectral signatures assigned to it, the classifier can assign areas with related

land cover types to “Woody”. Thus, it was concluded to test different variations of the LUCAS data set.

Therefore, the study compared four different variations of LUCAS data used: Firstly, an unmodified version. Secondly a version with added samples to support small classes (such as “Water” and “Non-vegetated unsealed surfaces”) and counterbalance issues detected within the first stages of the study. Thirdly, two versions with a limited class definition of “Woody” class, which means that LUCAS subclasses including agriculture and shrubland were removed. One was tested with and the other one without additional sampling to better define dark forest canopy. ´

The unmodified LUCAS dataset resulted in the classification with the lowest accuracy of the four approaches with a difference of 10% to the best prediction result of 62%. The second lowest accuracy was achieved by the classification with additional sampling and a broad “Woody” class. The two highest accuracies were achieved by classifications where agricultural related classes such as orchards and vineyards from “Woody” were removed. This indicates that misclassifications were caused by the nomenclature definition, as explained above.

The comparison between the two classifications with a limited “Woody” class definition indicated another source of inaccuracy when conducting a classification solely based on LUCAS training data. The data set version including extra samples to distinguish dark forest canopy and water reached a 1% higher overall accuracy than the one without. It was thus shown that even though “Woody” is the largest and most dominant class in the training set, certain spectral signatures are still not represented enough to provide sufficient information to the classifier to distinguish between water and dark forest canopy. Thus, the class size does not necessarily indicate that all relevant spectral signatures and its connected classes are sufficiently represented in the LUCAS 2015 data set for Central Portugal.

Regarding the second research question of this study on assessing the usability of LUCAS as training data for land cover classifications with classifications algorithms, it was concluded that the use of an unmodified training set solely based on LUCAS

results in overall low accuracy of the classification in this study, and it is thus not recommended as a sole substitute for selecting training areas by photointerpretation. This is caused by an unbalanced training set with a wide range in class size and the issues of remote assessment of points by surveyors, uncertainties caused by the LUCAS survey protocol, and the problem of misclassifications by the surveyors. The accuracy assessment of the data set variations confirmed the need for additional samples and ancillary data to produce predictions with high accuracy.

Considering that using LUCAS data comes with a variety of uncertainties and possible sources of error, it is hypothesised that the classifications conducted would have resulted in higher accuracy when using a larger, more balanced and more precise data set for training the classifier and a more narrowly defined nomenclature.

6.1. Contributions

The contributions made by this study can be divided into the two research questions stated at the beginning of the thesis: Compare and assess the two classification approaches, and testing the usability of LUCAS data as training data for a classifier.

Regarding the classification approaches of multi-temporal, multi-spectral Sentinel-2 data within one classification process in Random Forest, it can be said that this study was an addition to a comparably small amount of literature on the topic. It further investigated the ways and abilities of RF as a classifier to handle these types of multi-temporal classifications. The results of the study indicate potential for further research regarding the approach based on 100 bands, and furthermore a need to improve the classification approach based on the single month maps. Regarding the usability assessment of the LUCAS data as training data set for land cover classification maps, this study is contributing the highlighting of issues in the classification caused by issues in data collection process and protocol as defined by EUROSTAT. Most of these issues were already discussed within the literature, yet were not focussed within one study and tested based on a variety of modified LUCAS datasets. Mack et al. (2017) stated that a specific issue to investigate is the usability of LUCAS data as a training data base for supervised classification approaches, which is one of the core objectives of this study manged to do.

6.2. Limitations and Recommendations

This study highlighted its limitations extensively in the discussion section. The limitations include a too broad definition of the "Woody" class, leading to many misclassifications within all approaches used. The training data in all variations was unbalanced, causing difficulties for the classifier to correctly identify land cover types and thus reduced the accuracy. Additionally, the difference of using training data collected in 2015 to classify imagery from end of 2016 until end of 2017 could have led to a reduction in accuracies of the classifications conducted. It would be of interest to repeat the study with a more balanced and bigger dataset for training which was collected in the same year as the aerial imagery. An opportunity for this would the release of the new LUCAS data set in 2018.

Common issues known in the field of remote sensing should also be taken into consideration. These include the "Salt-and-Pepper" effect, which was increased by choosing a hard classification approach. This approach does not deal with the mixed-pixel problem which is caused by the co-existence of different land cover types in the same pixel. A study based on a fuzzy classification method is recommended to be conducted to further investigate the issue.

Moreover, it was concluded that the approach based on the single month maps achieved a significantly lower accuracy than the approach based on 100 bands. A possible explanation for the low accuracy of the map based on the single month maps is that misclassifications of land cover types conducted in the single month maps were transferred into the final map. A recommended topic for future studies is to analyse and assess this possibility by composing testing data sets for each single month map to identify and track misclassifications.

Overall, the approach based on the single classification of a stack of multi-temporal, multi-spectral bands showed potential and should be analysed in further studies. In conclusion, it would be advisable to repeat the study with a larger, more balanced and current training data set (possibly LUCAS 2018 with added samples or ancillary data) and redefined classes in the nomenclature, which reflects the land cover classes more clearly.

BIBLIOGRAPHIC REFERENCES

ALCANTARA, C., KUEMMERLE, T., PRISHCHEPOV, A. V., & RADELOFF, V. C. (2012). Mapping abandoned agriculture with multi-temporal MODIS satellite data. *Remote Sensing of Environment*, *124*, pp. 334–347. (URL: https://doi.org/10.1016/j.rse.2012.05.019 Retrieved 23-11-2017)

ATZBERGER, C., & EILERS, P. H. C. (2011). A time series for monitoring vegetation activity and phenology at 10-daily time steps covering large parts of South America. *International Journal of Digital Earth*, *4*(5), pp. 365–386. (URL: https://doi.org/10.1080/17538947.2010.505664 Retrieved 23-12-2017)

BELGIU, M., & DRA, L. (2016). Random forest in remote sensing : A review of applications and future directions. *ISPRS Journal of Photogrammetry and Remote Sensing*, *114*, pp. 24–31. (URL: https://doi.org/10.1016/j.isprsjprs.2016.01.011 Retrieved 18-12-2017)

BELGIU, M., DRĂGUŢ, L., & STROBL, J. (2014). Quantitative evaluation of variations in rule-based classifications of land cover in urban neighbourhoods using WorldView-2 imagery. *ISPRS Journal of Photogrammetry and Remote Sensing*, *87*, pp. 205–215. (URL: https://doi.org/10.1016/j.isprsjprs.2013.11.007 Retrieved 23-11-2017)

BLASCHKE, T. (2010). Object based image analysis for remote sensing. *ISPRS Journal of Photogrammetry and Remote Sensing*, *65*(1), pp. 2–16. (URL: https://doi.org/10.1016/j.isprsjprs.2009.06.004 Retrieved 07-01-2018)

BREIMAN, L. (2001). Random forests. *Machine Learning*, (45), pp. 5–32. (URL: https://doi.org/10.1017/CBO9781107415324.004 Retrieved 20-01-2018)

BREIMAN, L., & CUTLER, A. (2015). Breiman and Cutler's Random Forests for Classification and Regression 4.6-12. (URL: https://doi.org/10.1015/CBO7861107415324.004 Retrieved 07-01-2018)

CAMPBELL, J. B. (1996). *Introduction to remote sensing* (2nd ed.). London: Taylor & Francis.

CÁNOVAS-GARCÍA, F., ALONSO-SARRÍA, F., & GOMARIZ-CASTILLO, F. (2017). Modification of the random forest algorithm to avoid statistical dependence problems when classifying remote sensing imagery. *Computers and*

Geosciences, *103*(September 2016), pp. 1–11. (URL: https://doi.org/10.1016/j.cageo.2017.02.012 Retrieved 20-12-2017)

CANTERS, F. (1997). Evaluating the uncertainty of area estimates derived from fuzzy land-cover classification. *Photogrammetric Engineering & Remote Sensing*, *63*(4), pp. 403–414. (URL: https://doi.org/10.1.1.458.4408 Retrieved 20-12-2017)

CHEN, X., VIERLING, L., & DEERING, D. (2005). A simple and effective radiometric correction method to improve landscape change detection across sensors and across time. *Remote Sensing of Environment*, *98*(1), pp. 63–79. (URL: https://doi.org/10.1016/j.rse.2005.05.021 Retrieved 14-11-2017)

CIESLAK, D. A., & CHAWLA, N. V. (2008). Learning decision trees for unbalanced data. *Lecture Notes in Computer Science*, *5211 LNAI*(PART 1), pp. 241–256. (URL: https://doi.org/10.1007/978-3-540-87479-9_34 Retrieved 07-01-2018)

CLARK, M. L. (2017). Comparison of simulated hyperspectral HyspIRI and multispectral Landsat 8 and Sentinel-2 imagery for multi-seasonal, regional land-cover mapping. *Remote Sensing of Environment*, *200*(August), pp. 311–325. (URL: https://doi.org/10.1016/j.rse.2017.08.028 Retrieved 08-01-2018)

CLARK, M. L., AIDE, T. M., & RINER, G. (2012). Land change for all municipalities in Latin America and the Caribbean assessed from 250-m MODIS imagery (2001-2010). *Remote Sensing of Environment*, *126*, pp. 84–103. (URL: https://doi.org/10.1016/j.rse.2012.08.013 Retrieved 08-01-2018)

CLEVERS, J., & GITELSON, A. A. (2013). Remote estimation of crop and grass chlorophyll and nitrogen content using red-edge bands on Sentinel-2 and -3. *International Journal of Applied Earth Observation and Geoinformation*, *23*(1), pp. 334–351. (URL: https://doi.org/10.1016/j.jag.2012.10.008 Retrieved 14-12-2017)

CONGALTON, R. G. (1991). A review of assessing the accuracy of classifications of remotely sensed data. *Remote Sensing of Environment*, *37*(1), pp. 35–46. (URL: https://doi.org/10.1016/0034-4257(91)90048-B Retrieved 11-12-2017)

CONGALTON, R. G., & GREEN, K. (1993). A practical look at the sources of confusion in error matrix generation. *Photogrammetric Engineering & Remote Sensing*,

59(5), pp. 641–644. (URL: https://doi.org/10.1018/0034-4257(91)90048-C Retrieved 11-12-2017)

COPERNICUS. (2017). Open Access Hub. (URL: https://scihub.copernicus.eu/ Retrieved 15-12-2017)

DE MATTEIS, A. D., MARCELLONI, F., & SEGATORI, A. (2015). A new approach to fuzzy random forest generation. *IEEE International Conference on Fuzzy Systems*, *2015–Novem*. (URL: https://doi.org/10.1109/FUZZ-IEEE.2015.7337919 Retrieved 20-11-2017)

DEREN, L., HAIGANG, S., & PING, X. (2003). Automatic change detection of geo-spatial data from imagery. *Geo-Spatial Information Science*, *6*(3), pp. 1–7. (URL: https://doi.org/10.1007/BF02826885 Retrieved 20-12-2017)

DGT. (2017). CAOP- Carta Administrativa Oficial de Portugal. (URL: www.dgterritorio.pt/cartografia_e_geodesia/cartografia/carta_administrativa_oficial_de_portugal_caop_/caop_download_/ Retrieved 06-02-2018)

DONG, T., MENG, J., SHANG, J., LIU, J., & WU, B. (2015). Evaluation of Chlorophyll-Related Vegetation Indices Using Simulated Sentinel-2 Data for Estimation of Crop Fraction of Absorbed Photosynthetically Active Radiation. *IEEE Journal of Selected Topics in Applied Earth Observations and Remote Sensing*, *8*(8), pp. 4049–4059. (URL: https://doi.org/10.1109/JSTARS.2015.2400134 Retrieved 20-12-2017)

DRUSCH, M., DEL BELLO, U., CARLIER, S., COLIN, O., FERNANDEZ, V., GASCON, F., BARGELLINI, P. (2012). Sentinel-2: ESA's Optical High-Resolution Mission for GMES Operational Services. *Remote Sensing of Environment*, *120*, pp. 25–36. (URL: https://doi.org/10.1016/j.rse.2011.11.026 Retrieved 20-01-2017)

DU, Y., ZHANG, Y., LING, F., WANG, Q., LI, W., & LI, X. (2016). Water bodies' mapping from Sentinel-2 imagery with Modified Normalized Difference Water Index at 10-m spatial resolution produced by sharpening the swir band. *Remote Sensing*, *8*(4). (URL: https://doi.org/10.3390/rs8040354 Retrieved 20-01-2017)

EC. (2017). Land Cover/Use Statistics (LUCAS) Overview. (URL: http://ec.europa.eu/eurostat/web/lucas Retrieved 16-11-2017)

EISAVI, V., HOMAYOUNI, S., YAZDI, A. M., & ALIMOHAMMADI, A. (2015). Land cover

mapping based on random forest classification of multitemporal spectral and thermal images. *Environmental Monitoring and Assessment*, *187*(5), pp. 1–14. (URL: https://doi.org/10.1007/s10661-015-4489-3 Retrieved 20-11-2017)

ESA. (2017a). Data Products. (URL: http://www.esa.int/Our_Activities/Observing_the_Earth/Copernicus/Sentinel-2/Data_products Retrieved 16-12-2017)

ESA. (2017b). Facts and Figures. (URL: http://m.esa.int/Our_Activities/Observing_the_Earth/Copernicus/Sentinel-2/Facts_and_figures Retrieved 19-11-2017)

ESA. (2017c). Radiometric Resolutions. (URL: https://earth.esa.int/web/sentinel/user-guides/sentinel-2-msi/resolutions/radiometric Retrieved 05-11-2017)

ESA. (2017d). Sen2Cor. (URL: http://step.esa.int/main/third-party-plugins-2/sen2cor/ Retrieved 19-11-2017)

ESA. (2017e). Sen2Cor Algorithm. (URL: https://sentinel.esa.int/web/sentinel/technical-guides/sentinel-2-msi/level-2a/algorithm Retrieved 17-11-2017)

ESA. (2017f). The Sentinel-2 Toolbox. (URL: https://sentinel.esa.int/web/sentinel/toolboxes/sentinel-2 Retrieved 15-11-2017)

ESAU, I., MILES, V. V., DAVY, R., MILES, M. W., & KURCHATOVA, A. (2016). Trends in normalized difference vegetation index (NDVI) associated with urban development in northern West Siberia. *Atmospheric Chemistry and Physics*, *16*(15), pp. 9563–9577. (URL: https://doi.org/10.5194/acp-16-9563-2016 Retrieved 20-11-2017)

ESCH, T., METZ, A., MARCONCINI, M., & KEIL, M. (2014). Combined use of multi-seasonal high and medium resolution satellite imagery for parcel-related mapping of cropland and grassland. *International Journal of Applied Earth Observation and Geoinformation*, *28*(1), pp. 230–237. (URL: https://doi.org/10.1016/j.jag.2013.12.007 Retrieved 20-12-2017)

EUROSTAT. (2016). *LUCAS SURVEY2015 WEB CSV Record Descriptor*. (URL: http://ec.europa.eu/eurostat/documents/205002/6786255/WebCsv_RecordDescri

ptor20161006.pdf Retrieved 02-01-2018)

EUROSTAT. (2017). Technical reference document C3- Classification (Land cover & Land use). (URL: http://ec.europa.eu/eurostat/documents/205002/6786255/LUCAS2015-C3-Classification-20150227.pdf/969ca853-e325-48b3-9d59-7e86023b2b27 Retrieved 05-11-2017)

FAGAN, M. E., DEFRIES, R. S., SESNIE, S. E., ARROYO-MORA, J. P., SOTO, C., SINGH, A., CHAZDON, R. L. (2015). Mapping species composition of forests and tree plantations in northeastern Costa Rica with an integration of hyperspectral and multitemporal landsat imagery. *Remote Sensing*, *7*(5), pp. 5660–5696. (URL: https://doi.org/10.3390/rs70505660 Retrieved 20-12-2017)

FERNÁNDEZ-MANSO, A., FERNÁNDEZ-MANSO, O., & QUINTANO, C. (2016). SENTINEL-2A red-edge spectral indices suitability for discriminating burn severity. *International Journal of Applied Earth Observation and Geoinformation*, *50*, pp. 170–175. (URL: https://doi.org/10.1016/j.jag.2016.03.005 Retrieved 20-12-2017)

FOODY, G. M. (2002). Status of land cover classification accuracy assessment. *Remote Sensing of Environment*, *80*(1), pp. 185–201. (URL: https://doi.org/10.1016/S0034-4257(01)00295-4 Retrieved 20-11-2017)

GALLEGO, F. J. (2011). Validation of GIS layers in the EU: Getting adapted to available reference data. *International Journal of Digital Earth*, *4*(SUPPL. 1), pp. 42–57. (URL: https://doi.org/10.1080/17538947.2010.512746 Retrieved 20-12-2017)

GARDI, C., & YIGINI, Y. (2012). Continuous Mapping of Soil pH Using Digital Soil Mapping Approach in Europe. *Eurasian Journal of Soil Science*, *2*, pp. 64–68. (URL: https://doi.org/10.1015/17538947.2011.512746 Retrieved 15-12-2017)

GESSNER, U., MACHWITZ, M., ESCH, T., TILLACK, A., NAEIMI, V., KUENZER, C., & DECH, S. (2015). Multi-sensor mapping of West African land cover using MODIS, ASAR and TanDEM-X/TerraSAR-X data. *Remote Sensing of Environment*, *164*, pp. 282–297. (URL: https://doi.org/10.1016/j.rse.2015.03.029 Retrieved 17-11-2017)

GISINTERNALS. (2017). GDAL 202 Stable Release. (URL: http://www.gisinternals.com/release.php Retrieved 15-11-2017)

GISLASON, P. O., BENEDIKTSSON, J. A., & SVEINSSON, J. R. (2006). Random forests for land cover classification. *Pattern Recognition Letters*, *27*(4), pp. 294–300. (URL: https://doi.org/10.1016/j.patrec.2005.08.011 Retrieved 20-01-2017)

GONG, P., WANG, J., YU, L., ZHAO, Y., ZHAO, Y., LIANG, L.,CHEN, J. (2013). Finer resolution observation and monitoring of global land cover: First mapping results with Landsat TM and ETM+ data. *International Journal of Remote Sensing*, *34*(7), pp. 2607–2654. (URL: https://doi.org/10.1080/01431161.2012.748992 Retrieved 09-01-2017)

GU, Y., BROWN, J. F., MIURA, T., VAN LEEUWEN, W. J. D., & REED, B. C. (2010). Phenological classification of the United States: A geographic framework for extending multi-sensor time-series data. *Remote Sensing*, *2*(2), pp. 526–544. (URL: https://doi.org/10.3390/rs2020526 Retrieved 14-01-2017)

HAY, A. M. (1988). Remote sensing letters the derivation of global estimates from a confusion matrix. *International Journal of Remote Sensing*, *9*(8), pp. 1395–1398. (URL: https://doi.org/10.1080/01431168808954945 Retrieved 14-01-2017)

HIJMANS, R., VAN ETTEN, J., CHENG, J., MATTIUZZI, M., GREENBERG, J., BEVAN, A., GHOSH, A. (2017). raster 2.6-7 - Geographic Data Analysis and Modeling. (URL: https://cran.r-project.org/web/packages/raster/raster.pdf Retrieved 17-12-2017)

HOMER, C., DEWITZ, J., FRY, J., COAN, M., HOSSAIN, N., LARSON, C., WICKHAM, J. (2007). Completion of the 2001 National Land Cover Database for the Conterminous United States. *PHOTOGRAMMETRIC ENGINEERING & REMOTE SENSING*, *73*(4), pp. 337–341. (URL: https://pubs.er.usgs.gov/publication/70029996 Retrieved 22-11-2017)

IM, J., RHEE, J., JENSEN, J. R., & HODGSON, M. E. (2007). An automated binary change detection model using a calibration approach. *Remote Sensing of Environment*, *106*(1), pp. 89–105. (URL: https://doi.org/10.1016/j.rse.2006.07.019 Retrieved 03-12-2017)

IMMITZER, M., VUOLO, F., & ATZBERGER, C. (2016). First experience with Sentinel-2 data for crop and tree species classifications in central Europe. *Remote Sensing*,

8(3). (URL: https://doi.org/10.3390/rs8030166 Retrieved 11-11-2017)

INGLADA, J., ARIAS, M., TARDY, B., HAGOLLE, O., VALERO, S., MORIN, D., KOETZ, B. (2015). Assessment of an operational system for crop type map production using high temporal and spatial resolution satellite optical imagery. *Remote Sensing*, *7*(9), pp. 12356–12379. (URL: https://doi.org/10.3390/rs70912356 Retrieved 17-12-2017)

JIA, K., LIANG, S., WEI, X., YAO, Y., SU, Y., JIANG, B., & WANG, X. (2014). Land cover classification of landsat data with phenological features extracted from time series MODIS NDVI data. *Remote Sensing*, *6*(11), pp. 11518–11532. (URL: https://doi.org/10.3390/rs61111518 Retrieved 17-12-2017)

JIA, K., LIANG, S., ZHANG, N., WEI, X., GU, X., ZHAO, X., XIE, X. (2014). Land cover classification of finer resolution remote sensing data integrating temporal features from time series coarser resolution data. *ISPRS Journal of Photogrammetry and Remote Sensing*, *93*, pp. 49–55. (URL: https://doi.org/10.1016/j.isprsjprs.2014.04.004 Retrieved 24-12-2017)

JIMÉNEZ-VALVERDE, A., & LOBO, J. M. (2006). The ghost of unbalanced species distribution data in geographical model predictions. *Diversity and Distributions*, *12*(5), pp. 521–524. (URL: https://doi.org/10.1111/j.1366-9516.2006.00267.x Retrieved 05-12-2017)

JUPP, D. L. B. (1989). The stability of global estimates from confusion matrices. *International Journal of Remote Sensing*, *10*(9), pp. 1563–1569. (URL: https://doi.org/10.1080/01431168908903990 Retrieved 18-12-2017)

JUSTICE, B. O., & HIERNAUX, P. H. Y. (1986). Monitoring the grasslands of the sahel using NOAA AVHRR data: Niger 1983. *International Journal of Remote Sensing*, *7*(11), pp. 1475–1497. (URL: https://doi.org/10.1080/01431168608948949 Retrieved 14-12-2017)

KARLSON, M., OSTWALD, M., REESE, H., SANOU, J., TANKOANO, B., & MATTSSON, E. (2015). Mapping tree canopy cover and aboveground biomass in Sudano-Sahelian woodlands using Landsat 8 and random forest. *Remote Sensing*, *7*(8), pp. 10017–10041. (URL: https://doi.org/10.3390/rs70810017 Retrieved 18-12-2017)

KARYDAS, C. G., GITAS, I. Z., KUNTZ, S., & MINAKOU, C. (2015). Use of LUCAS LC point database for validating country-scale land cover maps. *Remote Sensing*, *7*(5), pp. 5012–5041. (URL: https://doi.org/10.3390/rs70505012 Retrieved 18-12-2017)

KORHONEN, L., HADI, PACKALEN, P., & RAUTIAINEN, M. (2017). Comparison of Sentinel-2 and Landsat 8 in the estimation of boreal forest canopy cover and leaf area index. *Remote Sensing of Environment*, *195*, pp. 259–274. (URL: https://doi.org/10.1016/j.rse.2017.03.021 Retrieved 14-12-2017)

KUHN, M. (2017). Caret 6.0-78 - Classification and Regression Training. (URL: caret.r-forge.r-project.org Retrieved 15-12-2017)

KUSSUL, N., LAVRENIUK, M., SKAKUN, S., & SHELESTOV, A. (2017). Deep Learning Classification of Land Cover and Crop Types Using Remote Sensing Data. *IEEE Geoscience and Remote Sensing Letters*, *14*(5), pp. 778–782. (URL: https://doi.org/10.1109/LGRS.2017.2681128 Retrieved 08-01-2017)

LAMBIN, E. F., & LINDERMAN, M. (2006). Time series of remote sensing data for land change science. *Geoscience and Remote Sensing, IEEE Transactions*, *44*(7), pp. 1926–1928. (URL: https://doi.org/10.1109/tgrs.2006.872932 Retrieved 14-12-2017)

LAWRENCE, R. L., & MORAN, C. J. (2015). The AmericaView classification methods accuracy comparison project: A rigorous approach for model selection. *Remote Sensing of Environment*, *170*, pp. 115–120. (URL: https://doi.org/10.1016/j.rse.2015.09.008 Retrieved 08-11-2017)

LAWRENCE, R. L., WOOD, S. D., & SHELEY, R. L. (2006). Mapping invasive plants using hyperspectral imagery and Breiman Cutler classifications (randomForest). *Remote Sensing of Environment*, *100*(3), pp. 356–362. (URL: https://doi.org/10.1016/j.rse.2005.10.014 Retrieved 09-12-2017)

LI, M., MA, L., BLASCHKE, T., CHENG, L., & TIEDE, D. (2016). A systematic comparison of different object-based classification techniques using high spatial resolution imagery in agricultural environments. *International Journal of Applied Earth Observations and Geoinformation*, *49*, pp. 87–98. (URL: https://doi.org/10.1016/j.jag.2016.01.011 Retrieved 14-12-2017)

LOUIS, J., DEBAECKER, V., PFLUG, B., MAIN-KNORN, M., & BIENIARZ, J. (2016). Sentinel-Sen2Cor, *Living Planet Symposium 2016*, Prague (URL: http://elib.dlr.de/107381/1/LPS2016_sm10_3louis.pdf Retrieved 27-11-2017)

LU, D., LI, G., MORAN, E., & HETRICK, S. (2013). Spatiotemporal analysis of land-use and land-cover change in the Brazilian Amazon. *International Journal of Remote Sensing*, *34*(16), pp. 5953–5978. (URL: https://doi.org/10.1080/01431161.2013.802825 Retrieved 10-12-2017)

MACK, B., LEINENKUGEL, P., KUENZER, C., & DECH, S. (2017). A semi-automated approach for the generation of a new land use and land cover product for Germany based on Landsat time-series and Lucas in-situ data. *Remote Sensing Letters*, *8*(3), pp. 244–253. (URL: https://doi.org/10.1080/2150704X.2016.1149299 Retrieved 14-12-2017)

MALENOVSKÝ, Z., ROTT, H., CIHLAR, J., SCHAEPMAN, M. E., GARCÍA-SANTOS, G., FERNANDES, R., & BERGER, M. (2012). Sentinels for science: Potential of Sentinel-1, -2, and -3 missions for scientific observations of ocean, cryosphere, and land. *Remote Sensing of Environment*, *120*, pp. 91–101. (URL: https://doi.org/10.1016/j.rse.2011.09.026 Retrieved 14-11-2017)

MATSUSHITA, B., YANG, W., CHEN, J., ONDA, Y., & QIU, G. (2007). Sensitivity of the Enhanced Vegetation Index (EVI) and Normalized Difference Vegetation Index (NDVI) to topographic effects: A case study in high-density cypress forest. *Sensors*, *7*(11), pp. 2636–2651. (URL: https://doi.org/10.3390/s7112636 Retrieved 18-11-2017)

NAVARRO, G., CABALLERO, I., SILVA, G., PARRA, P.-C., VÁZQUEZ, Á., & CALDEIRA, R. (2017). Evaluation of forest fire on Madeira Island using Sentinel-2A MSI imagery. *International Journal of Applied Earth Observation and Geoinformation*, *58*, pp. 97–106. (URL: https://doi.org/10.1016/j.jag.2017.02.003 Retrieved 18-12-2017)

NEVES, A. K., BENDINI, H. N., KÖRTING, T. S., & FONSECA, L. M. G. (2015). Combining Time Series Features and Data Mining to Detect Land Cover patterns : a Case Study in Northern Mato Grosso. In *Proceedings XVI GEOINFO* (pp. 174–185). (URL: https://doi.org/ 10.13140/RG.2.1.3494.2807 Retrieved 18-12-2017)

NITZE, I., BARRETT, B., & CAWKWELL, F. (2015). Temporal optimisation of image acquisition for land cover classification with random forest and MODIS time-series. *International Journal of Applied Earth Observation and Geoinformation*, *34*(1), pp. 136–146. (URL: https://doi.org/10.1016/j.jag.2014.08.001 Retrieved 10-11-2017)

NOVELLI, A., AGUILAR, M. A., NEMMAOUI, A., AGUILAR, F. J., & TARANTINO, E. (2016). Performance evaluation of object based greenhouse detection from Sentinel-2 MSI and Landsat 8 OLI data: A case study from Almería (Spain). *International Journal of Applied Earth Observation and Geoinformation*, *52*, pp. 403–411. (URL: https://doi.org/10.1016/j.jag.2016.07.011 Retrieved 10-11-2017)

PAL, M. (2005). Random forest classifier for remote sensing classification. *International Journal of Remote Sensing*, *26*(1), pp. 217–222. (URL: https://doi.org/10.1080/01431160412331269698 Retrieved 15-12-2017)

PANAGOS, P., MEUSBURGER, K., BALLABIO, C., BORRELLI, P., & ALEWELL, C. (2014). Soil erodibility in Europe: A high-resolution dataset based on LUCAS. *Science of the Total Environment*, *479–480*(1), pp. 189–200. (URL: https://doi.org/10.1016/j.scitotenv.2014.02.010 Retrieved 20-11-2017)

PELLETIER, C., VALERO, S., INGLADA, J., CHAMPION, N., & DEDIEU, G. (2016). Assessing the robustness of Random Forests to map land cover with high resolution satellite image time series over large areas. *Remote Sensing of Environment*, *187*, pp. 156–168. (URL: https://doi.org/10.1016/j.rse.2016.10.010 Retrieved 08-11-2017)

PONTIUS, R. G. (2000). Quantification error versus location error in comparison of categorical maps. *Photogrammetric Engineering and Remote Sensing*. (URL: https://www.clarku.edu/~rpontius/pontius_2000_pers.pdf Retrieved 13-02-2018)

R. (2017). R Studio 3.4.2 (64-bit). Retrieved from https://www.r-project.org/

RAMOELO, A., CHO, M., MATHIEU, R., & SKIDMORE, A. K. (2015). Potential of Sentinel-2 spectral configuration to assess rangeland quality. *Journal of Applied Remote Sensing*, *9*(1), pp. 94096. (URL: https://doi.org/10.1117/1.JRS.9.094096 Retrieved 20-11-2017)

RODRIGUEZ-GALIANO, V. F., CHICA-OLMO, M., ABARCA-HERNANDEZ, F., ATKINSON, P. M., & JEGANATHAN, C. (2012). Random Forest classification of Mediterranean land cover using multi-seasonal imagery and multi-seasonal texture. *Remote Sensing of Environment*, *121*, pp. 93–107. (URL: https://doi.org/10.1016/j.rse.2011.12.003 Retrieved 07-01-2017)

RODRIGUEZ-GALIANO, V. F., GHIMIRE, B., ROGAN, J., CHICA-OLMO, M., & RIGOL-SANCHEZ, J. P. (2012). An assessment of the effectiveness of a random forest classifier for land-cover classification. *ISPRS Journal of Photogrammetry and Remote Sensing*, *67*, pp. 93–104. (URL: https://doi.org/10.1016/j.isprsjprs.2011.11.002 Retrieved 14-11-2017)

SCHMIDT, T., SCHUSTER, C., KLEINSCHMIT, B., & F??RSTER, M. (2014). Evaluating an intra-annual time series for grassland classification - How many acquisitions and what seasonal origin are optimal? *IEEE Journal of Selected Topics in Applied Earth Observations and Remote Sensing*, *7*(8), pp. 3428–3439. (URL: https://doi.org/10.1109/JSTARS.2014.2347203 Retrieved 28-12-2017)

SCHNEIDER, A. (2012). Monitoring land cover change in urban and peri-urban areas using dense time stacks of Landsat satellite data and a data mining approach. *Remote Sensing of Environment*, *124*, pp. 689–704. (URL: https://doi.org/10.1016/j.rse.2012.06.006 Retrieved 28-12-2017)

SCHUSTER, C., SCHMIDT, T., CONRAD, C., KLEINSCHMIT, B., & FÖRSTER, M. (2015). Grassland habitat mapping by intra-annual time series analysis -Comparison of RapidEye and TerraSAR-X satellite data. *International Journal of Applied Earth Observation and Geoinformation*, *34*(1), pp. 25–34. (URL: https://doi.org/10.1016/j.jag.2014.06.004 Retrieved 28-12-2017)

SINGH, A. (1989). Review Articlel: Digital change detection techniques using remotely-sensed data. *International Journal of Remote Sensing*, *10*(6), pp. 989–1003. (URL: https://doi.org/10.1080/01431168908903939 Retrieved 07-12-2017)

SMITS, P. C., DELLEPIANE, S. G., & SCHOWENGERDT, R. A. (1999). Quality assessment of image classification algorithms for land-cover mapping : A review and a proposal for a cost- based approach. *International Journal of Remote Sensing*, *20*(8), pp. 1461–1486. (URL: https://doi.org/10.1080/014311699212560

Retrieved 07-12-2017)

STEIDL, M. (2017). CadasterENV – User Meeting P1 : HR Land Cover Map. GeoVille. (Retrieved 05-11-2017)

STEPPER, C., STRAUB, C., & PRETZSCH, H. (2015). Using semi-global matching point clouds to estimate growing stock at the plot and stand levels : application for a broadleaf-dominated forest in central Europe. *Canadian Journal of Forest Research*, pp. 111–123. (URL: https://doi.org/10.1139/cjfr-2014-0297 Retrieved 20-11-2017)

STOW, D., HAMADA, Y., COULTER, L., & ANGUELOVA, Z. (2008). Monitoring shrubland habitat changes through object-based change identification with airborne multispectral imagery. *Remote Sensing of Environment*, *112*(3), pp. 1051–1061. (URL: https://doi.org/10.1016/j.rse.2007.07.011 Retrieved 20-11-2017)

STRATOULIAS, D., BALZTER, H., SYKIOTI, O., ZLINSZKY, A., & TÓTH, V. R. (2015). Evaluating sentinel-2 for lakeshore habitat mapping based on airborne hyperspectral data. *Sensors (Switzerland)*, *15*(9), pp. 22956–22969. (URL: https://doi.org/10.3390/s150922956 Retrieved 20-01-2017)

USGS. (2017). Raster Conversion Scripts. (URL: https://viewer.nationalmap.gov/tools/rasterconversion/Convert_JP2_Data_to_GeoTIFF_with_GDAL.html Retrieved 20-11-2017)

VAGLIO LAURIN, G., PULETTI, N., HAWTHORNE, W., LIESENBERG, V., CORONA, P., PAPALE, D., VALENTINI, R. (2016). Discrimination of tropical forest types, dominant species, and mapping of functional guilds by hyperspectral and simulated multispectral Sentinel-2 data. *Remote Sensing of Environment*, *176*, pp. 163–176. (URL: https://doi.org/10.1016/j.rse.2016.01.017 Retrieved 20-01-2017)

VAN DER MEER, F. D., VAN DER WERFF, H. M. A., & VAN RUITENBEEK, F. J. A. (2014). Potential of ESA's Sentinel-2 for geological applications. *Remote Sensing of Environment*, *148*, pp. 124–133. (URL: https://doi.org/10.1016/j.rse.2014.03.022 Retrieved 07-01-2017)

VAN DER SANDE, C. J., DE JONG, S. M., & DE ROO, A. P. J. (2003). A segmentation and

classification approach of IKONOS-2 imagery for land cover mapping to assist flood risk and flood damage assessment. *International Journal of Applied Earth Observation and Geoinformation*, *4*(3), pp. 217–229. (URL: https://doi.org/10.1016/S0303-2434(03)00003-5 Retrieved 18-12-2017)

VIERA, A. J., & GARRETT, J. M. (2005). Understanding Interobserver Agreement: The Kappa Statistic. *Family Medicine*, *37*(5), pp. 360–363. (URL: http://www1.cs.columbia.edu/~julia/courses/CS6998/Interrater_agreement.Kappa_statistic.pdf Retrieved 18-02-2018)

WANG, Q., SHI, W., LI, Z., & ATKINSON, P. M. (2016). Fusion of Sentinel-2 images. *Remote Sensing of Environment*, *187*, pp. 241–252. (URL: https://doi.org/10.1016/j.rse.2016.10.030 Retrieved 20-11-2017)

WARDLOW, B. D., & EGBERT, S. L. (2008). Large-area crop mapping using time-series MODIS 250 m NDVI data: An assessment for the U.S. Central Great Plains. *Remote Sensing of Environment*, *112*(3), pp. 1096–1116. (URL: https://doi.org/10.1016/j.rse.2007.07.019 Retrieved 15-12-2017)

YIN, H., PFLUGMACHER, D., KENNEDY, R. E., SULLA-MENASHE, D., & HOSTERT, P. (2014). Mapping Annual Land Use and Land Cover Changes Using MODIS Time Series. *Selected Topics in Applied Earth Observations and Remote Sensing, IEEE Journal of*, *7*(8), pp. 3421–3427. (URL: https://doi.org/10.1109/JSTARS.2014.2348411 Retrieved 07-12-2017)

ZHANG, X., FRIEDL, M. A., SCHAAF, C. B., STRAHLER, A. H., HODGES, J. C. F., GAO, F., HUETE, A. (2003). Monitoring vegetation phenology using MODIS. *Remote Sensing of Environment*, *84*(3), pp. 471–475. (URL: https://doi.org/10.1016/S0034-4257(02)00135-9 Retrieved 20-12-2017)

ZHAO, Y., FENG, D., YU, L., WANG, X., CHEN, Y., BAI, Y., GONG, P. (2016). Detailed dynamic land cover mapping of Chile: Accuracy improvement by integrating multi-temporal data. *Remote Sensing of Environment*, *183*, pp. 170–185. (URL: https://doi.org/10.1016/j.rse.2016.05.016 Retrieved 20-12-2017)

APPENDIX A - Single Month Maps

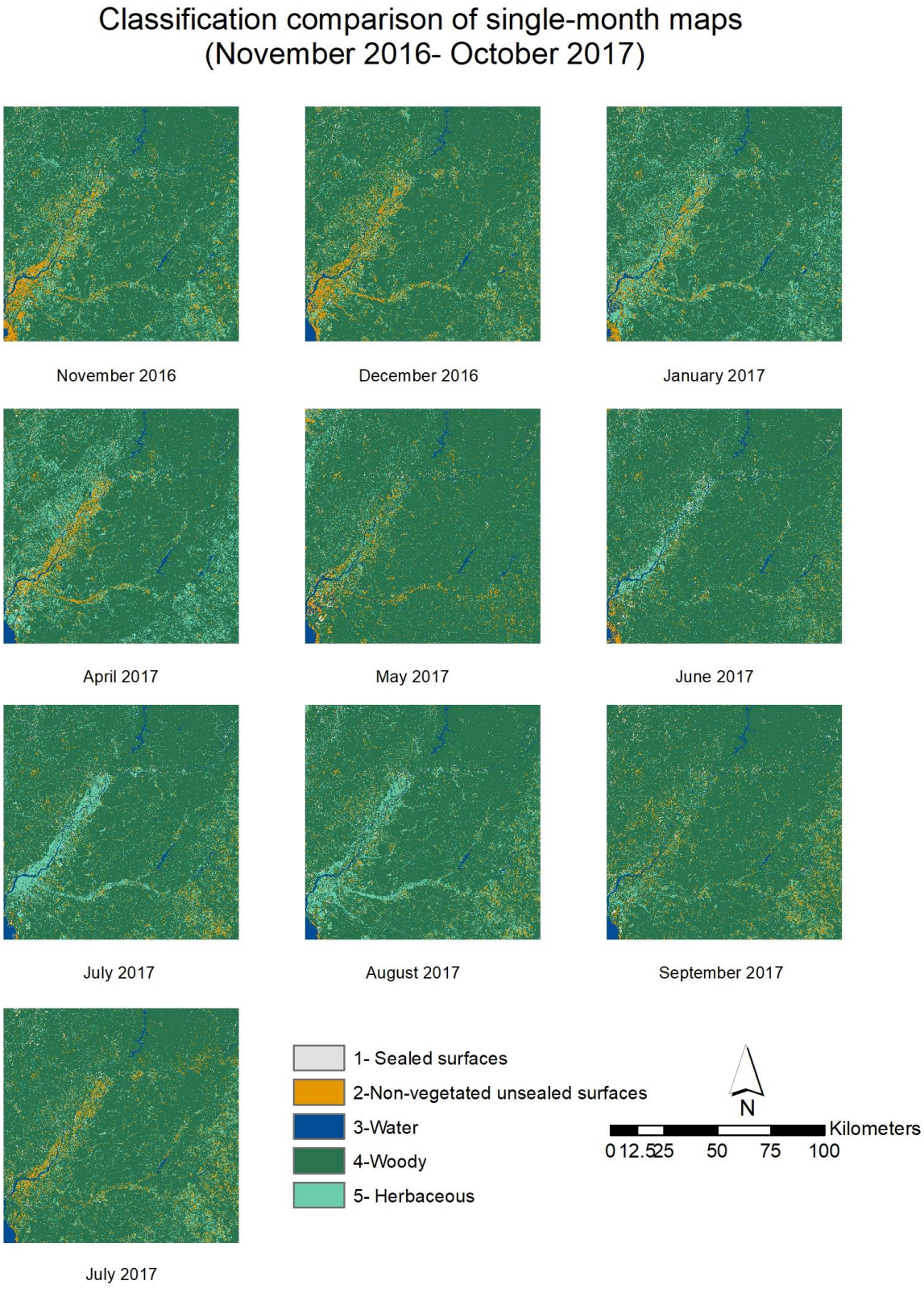

Classification of 10 single month maps

APPENDIX B – Additional Maps and Statistics

Mean	1114789.1	5642786.8	1786766.9	100672455.5	11343573.8
Standard Error	52063.76313	509486.5053	72895.03947	1116448.888	1138604.574
Median	1137679.5	5180783.5	1738949.5	100409421	11221145
Mode	#N/A	#N/A	#N/A	#N/A	#N/A
Standard Deviation	164640.075	1611137.794	230514.3549	3530521.378	3600583.807
Sample Variance	27106354309	2.59576E+12	53136867793	1.24646E+13	1.29642E+13
Kurtosis	0.165271752	-0.220014134	0.355498694	-1.188169419	-1.350788958
Skewness	-0.025277284	0.837933649	0.897197485	0.162420981	0.171385625
Range	548998	4797522	732378	10141381	10482245
Minimum	858094	3962777	1521855	95689898	6310507
Maximum	1407092	8760299	2254233	105831279	16792752
Sum	11147891	56427868	17867669	1006724555	113435738
Count	10	10	10	10	10

Exploratory analysis of “Sealed surfaces” to “Herbaceous periodic” based on single month maps

	Nov-16	Dec-16	Jan-17	Apr-17	May-17	Jun-17	Jul-17	Aug-17	Sep-17	Oct-17	AllMaps	AllBands Seed 5	AllBands Seed 17
Nov-16	1												
Dec-16	0,9987	1											
Jan-17	0,9989	0,9953	1										
Apr-17	0,9992	0,9960	0,9999	1									
May-17	0,9966	0,9988	0,9930	0,9942	1								
Jun-17	0,9978	0,9987	0,9952	0,9963	0,9997	1							
Jul-17	0,9994	0,9978	0,9988	0,9993	0,9974	0,9987	1						
Aug-17	0,9993	0,9976	0,9990	0,9995	0,9971	0,9985	1	1					
Sep-17	0,9978	0,9994	0,9945	0,9955	0,9998	0,9998	0,9981	0,9979	1				
Oct-17	0,9990	0,9998	0,9961	0,9969	0,9992	0,9994	0,9987	0,9985	0,9997	1			
AllMaps	0,9859	0,9892	0,9817	0,9836	0,9940	0,9935	0,9888	0,9885	0,9929	0,9906	1		
AllBands Seed 5	0,9924	0,9927	0,9908	0,9921	0,9958	0,9965	0,9950	0,9949	0,9954	0,9943	0,9980	1	
AllBands Seed 17	0,9927	0,9925	0,9914	0,9926	0,9954	0,9964	0,9953	0,9952	0,9952	0,9942	0,9975	1	1

Correlation table of all maps created

SURVEY_O_1	
Mean	99,92708
Standard Error	10,85272
Median	2
Mode	1
Standard Deviation	352,6715
Sample Variance	124377,2
Kurtosis	38,44202
Skewness	5,581689
Range	4124
Minimum	0
Maximum	4124
Sum	105523
Count	1056

Descriptive statistics of distance between in-situ point of LUCAS data and observation point

	1-Sealed surfaces	2-Non-vegetated unsealed surfaces	3-Water	4-Woody	5-Herbaceous (permanent)	(6-Herbaceous periodic)
LUCAS original	50	17	14	650	137	94
LUCAS post-sampling	50	51	53	671	137	94
Nov-16	50	90	53	671	192	
Dec-16	50	112	53	671	170	
Jan-17	50	72	53	671	210	
Apr-17	50	72	53	671	210	
May-17	50	90	53	671	192	
Jun-17	50	90	53	671	192	
Jul-17	50	84	53	671	198	
Aug-17	50	94	53	671	188	
Sep-17	50	103	53	671	179	
Oct-17	50	112	53	671	170	

Table of Sample Size per Class and Month

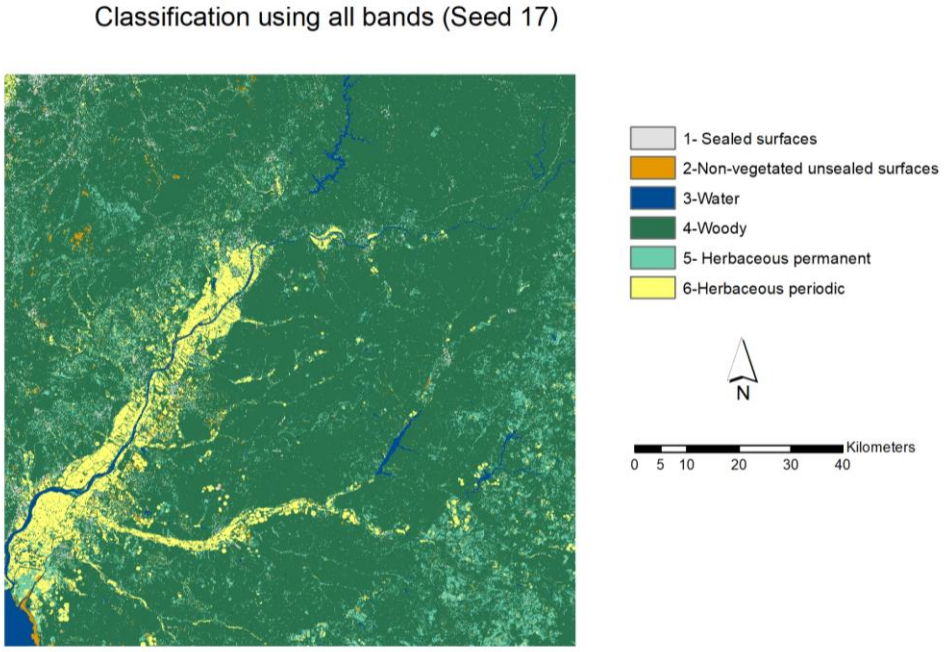

Land Cover Map using all bands in one classification process with Seed set to 17

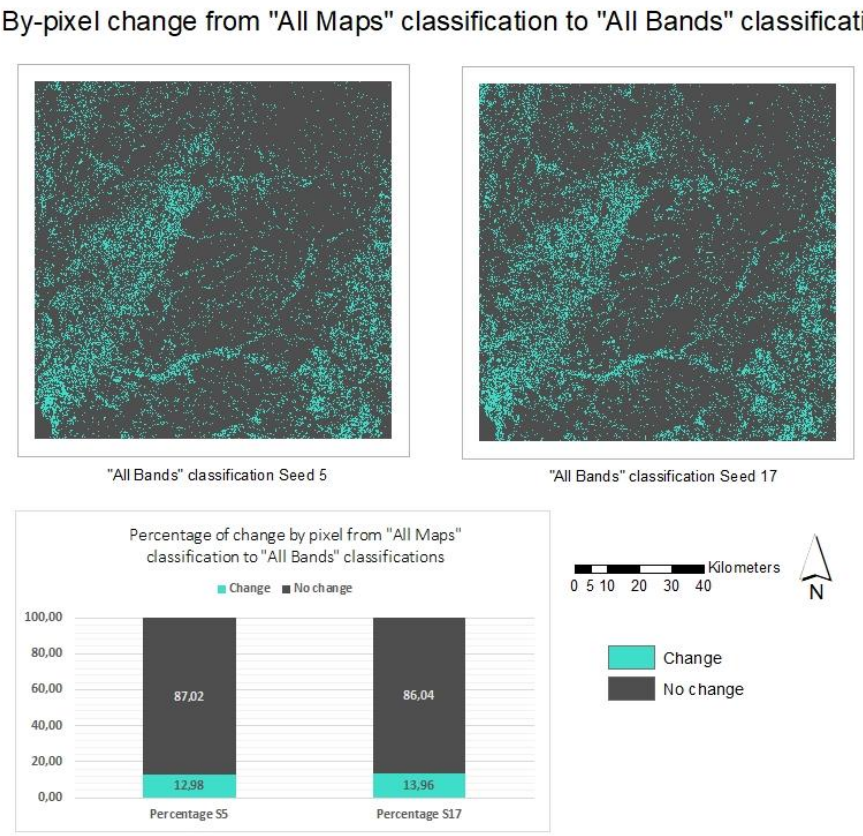

Binary Change Map using all bands in one classification process with Seed set to 5/ 17

	AllBands "Sealed surfaces"	**AllBands "Non-vegetated unsealed surfaces"**	**AllBands "Water"**	**AllBands "Woody "**	**AllBands "Herbaceous permanent"**	**AllBands "Herbaceous periodic"**
AllMaps "Sealed surfaces"	91,609	0,696	2,010	3,346	2,134	0,204
AllMaps "Non-vegetated unsealed surfaces"	2,774	92,939	1,774	1,113	0,831	0,569
AllMaps "Water"	0,865	0,345	98,099	0,457	0,173	0,061
AllMaps "Woody"	0,563	0,252	0,163	90,179	5,999	2,845
AllMaps "Herbaceous permanent"	4,428	0,366	4,732	24,372	42,223	23,879
AllMaps "Herbaceous periodic"	4,972	6,177	1,353	18,337	25,570	43,591

Percentage of class-to-class redistribution of pixels between classification approaches "AllMaps" and "AllBands" Seed 17

APPENDIX C – Codes in R

1. **Code for Single Month Maps ("1" / "tiff1" are exemplary for one month)**

```
# settings
#install.packages()

library(raster)
library(rgdal)
library(caret)

library(randomForest)

setwd("C:/Users/DaLued/Desktop/Thesis/Conversions/1/tiff1")

# import 10m TIFF images
files10=dir(pattern = "10m.*\\.tif$")
files10
image10=stack(files10)

#Downscale 20m resolution bands: Using raster package function
disaggregate
files20= dir(pattern = "20m.*\\.tif$")
files20

image20=stack(files20)
image20d= disaggregate(image20, fact=2)
image20d

#import ndvi from arc
ndvi=raster("ndvi1.tif")
ndvi

# Or calculate NDVI layer in R: (nir-red)/(nir+red) (B8-B4)/(B8+B4)
#ndvi2=((image10[[4]]-image10[[3]])/(image10[[4]]+image10[[3]]))

#Join image stacks
image=stack(image10,image20d)
image

# import LUCAS data
p=readOGR("C:/Users/DaLued/Desktop/Thesis/Conversions/1/tiff1","p3")
p=crop(p,image)
plot(image[[1]])
plot(p,add=T)

p$SURVEY_LC1
table(p$SURVEY_LC1)

# reclassify LUCAS to Austrian nomenclature
a=which(p$SURVEY_LC1==c("A11")|p$SURVEY_LC1==c("A21")|p$SURVEY_LC1==
c("A22"))
```

```
p@data[a,"austria"]="1"

b=which(p$SURVEY_LC1==c("F10")|p$SURVEY_LC1==c("F20")|p$SURVEY_LC1==
c("F40"))
p@data[b,"austria"]="2"

c=which(p$SURVEY_LC1==c("G11")|p$SURVEY_LC1==c("G21"))
p@data[c,"austria"]="3"

d=which(p$SURVEY_LC1==c("C10")|p$SURVEY_LC1==c("C22")|p$SURVEY_LC1==
c("C32")|p$SURVEY_LC1==c("C33")|p$SURVEY_LC1==c("D10")|p$SURVEY_LC1=
=c("D20")|p$SURVEY_LC1==c("B71")|p$SURVEY_LC1==c("B72")|p$SURVEY_LC1
==c("B73")|p$SURVEY_LC1==c("B74")|p$SURVEY_LC1==c("B75")|p$SURVEY_LC
1==c("B76")|p$SURVEY_LC1==c("B81")|p$SURVEY_LC1==c("B82")|p$SURVEY_L
C1==c("B83")|p$SURVEY_LC1==c("Bx2"))
p@data[d,"austria"]="4"

e=which(p$SURVEY_LC1==c("E10")|p$SURVEY_LC1==c("E20")|p$SURVEY_LC1==
c("E30"))
p@data[e,"austria"]="5"

f=which(p$SURVEY_LC1==c("B11")|p$SURVEY_LC1==c("B12")|p$SURVEY_LC1==
c("B15")|p$SURVEY_LC1==c("B16")|p$SURVEY_LC1==c("B17")|p$SURVEY_LC1=
=c("B18")|p$SURVEY_LC1==c("B19")|p$SURVEY_LC1==c("B21")|p$SURVEY_LC1
==c("B31")|p$SURVEY_LC1==c("B42")|p$SURVEY_LC1==c("B43")|p$SURVEY_LC
1==c("B53")|p$SURVEY_LC1==c("B54")|p$SURVEY_LC1==c("B55")|p$SURVEY_L
C1==c("Bx1"))
p@data[f,"austria"]="6"

table(p$austria)

#Split periodic herbaceous with ndvi threshold of 0.3 into bare land
and herbaceous
#copy p table
p$training=p$austria

#extract ndvi
ndvip=extract(ndvi,p)

p$ndvi=ndvip

#reassign classes to periodic points
h=which(p$ndvi<0.3& p$austria=="6")
p@data[h,"training"]="2"
g=which(p$ndvi>=0.3& p$austria=="6")
p@data[g,"training"]="5"

# Call new data table
p$training
table(p$training)
names(p)

# Extract pixel values to LUCAS points
values =extract(image,p)
```

```
# randomForest
ctrl = trainControl(method = "repeatedcv",repeats = 2)
randomForest.fit=train(x=values, y=p$training, method="rf",
ntree=500,tuneLength=10,trControl=ctrl)
# see fucntion 'randomForest' in package randomForest
plot(randomForest.fit)


# image classification
map=predict(image,randomForest.fit)
plot(map)
writeRaster(map,"map.tif",datatype="INT1U",overwrite=TRUE)
save.image("C:/Users/DaLued/Desktop/Thesis/Data/Sentinel/sentinel_en
vironment.RData")
```

2. **Code for Map based on Single Month Maps**

```
# settings
#install.packages()

library(raster)
library(rgdal)
library(caret)
library(randomForest)
library(snow)

setwd("C:/Users/DaLued/Desktop/Thesis/Conversions/map1")

# import maps
maps=list()
maps[[1]]=raster("C:/Users/DaLued/Desktop/Thesis/Conversions/map1.ti
f")
maps[[2]]=raster("C:/Users/DaLued/Desktop/Thesis/Conversions/map2.ti
f")
maps[[3]]=raster("C:/Users/DaLued/Desktop/Thesis/Conversions/map3.ti
f")
maps[[4]]=raster("C:/Users/DaLued/Desktop/Thesis/Conversions/map4.ti
f")
maps[[5]]=raster("C:/Users/DaLued/Desktop/Thesis/Conversions/map5.ti
f")
maps[[6]]=raster("C:/Users/DaLued/Desktop/Thesis/Conversions/map6.ti
f")
maps[[7]]=raster("C:/Users/DaLued/Desktop/Thesis/Conversions/map7.ti
f")
maps[[8]]=raster("C:/Users/DaLued/Desktop/Thesis/Conversions/map8.ti
f")
maps[[9]]=raster("C:/Users/DaLued/Desktop/Thesis/Conversions/map9.ti
f")
maps[[10]]=raster("C:/Users/DaLued/Desktop/Thesis/Conversions/map10.
tif")
```

```
# convert raster type to factor
for(i in 1:length(maps)){
  maps[[i]]=as.factor(maps[[i]])
}

#stack maps
maps=stack(maps)
projection(maps)=CRS("+proj=utm +zone=29 +datum=WGS84 +units=m
+no_defs +ellps=WGS84 +towgs84=0,0,0")

# import LUCAS data
p=readOGR("C:/Daria/Data/Sentinel/tiff1","p3")

# reclassify LUCAS to Austrian nomenclature
a=which(p$SURVEY_LC1==c("A11")|p$SURVEY_LC1==c("A21")|p$SURVEY_LC1==
c("A22"))
p@data[a,"austria"]="1"

b=which(p$SURVEY_LC1==c("F10")|p$SURVEY_LC1==c("F20")|p$SURVEY_LC1==
c("F40"))
p@data[b,"austria"]="2"

c=which(p$SURVEY_LC1==c("G11")|p$SURVEY_LC1==c("G21"))
p@data[c,"austria"]="3"

d=which(p$SURVEY_LC1==c("C10")|p$SURVEY_LC1==c("C22")|p$SURVEY_LC1==
c("C32")|p$SURVEY_LC1==c("C33")|p$SURVEY_LC1==c("D10")|p$SURVEY_LC1=
=c("D20")|p$SURVEY_LC1==c("B71")|p$SURVEY_LC1==c("B72")|p$SURVEY_LC1
==c("B73")|p$SURVEY_LC1==c("B74")|p$SURVEY_LC1==c("B75")|p$SURVEY_LC
1==c("B76")|p$SURVEY_LC1==c("B81")|p$SURVEY_LC1==c("B82")|p$SURVEY_L
C1==c("B83")|p$SURVEY_LC1==c("Bx2"))
p@data[d,"austria"]="4"

e=which(p$SURVEY_LC1==c("E10")|p$SURVEY_LC1==c("E20")|p$SURVEY_LC1==
c("E30"))
p@data[e,"austria"]="5"

f=which(p$SURVEY_LC1==c("B11")|p$SURVEY_LC1==c("B12")|p$SURVEY_LC1==
c("B15")|p$SURVEY_LC1==c("B16")|p$SURVEY_LC1==c("B17")|p$SURVEY_LC1=
=c("B18")|p$SURVEY_LC1==c("B19")|p$SURVEY_LC1==c("B21")|p$SURVEY_LC1
==c("B31")|p$SURVEY_LC1==c("B42")|p$SURVEY_LC1==c("B43")|p$SURVEY_LC
1==c("B53")|p$SURVEY_LC1==c("B54")|p$SURVEY_LC1==c("B55")|p$SURVEY_L
C1==c("Bx1"))
p@data[f,"austria"]="6"

p@data$austria=as.factor(p@data$austria)


# extract map values to LUCAS points
values=extract(maps,p,df=TRUE)
for (i in 2:ncol(values)){
  values[,i]=as.factor(values[,i])
}
values=values[,-1] # delete first column (Points' ID)
```

```
# fit randomForest with original package
randomForest.fit=randomForest(values, p$austria,mtry=10)

preds_rf=predict(maps,randomForest.fit)
writeRaster(preds_rf,"C:/Users/Daria/Desktop/Thesis/Conversions/map_
RF_randomForest_p3.tif",datatype="INT1U",overwrite=TRUE)
Sys.time()-time1


# multinominal classification for comparison
library(nnet)
multinom.fit=multinom(p$austria~., data=values)

time1=Sys.time()
beginCluster()
preds_rf = clusterR(maps, raster::predict, args = list(model =
multinom.fit))
endCluster()
writeRaster(preds_rf,"C:/Users/Daria/Desktop/Thesis/Conversions/map_
regression_multinom_p3.tif",datatype="INT1U",overwrite=TRUE)
Sys.time()-time1
```

3. Code for Map based on Classification of 100 Bands

```
# settings

#install.packages()
library(raster)
library(rgdal)
library(caret)
library(e1071)
library(randomForest)

setwd("C:/Users/Daria/Desktop/Thesis/tiffs")

# import 10m TIFF images
files10=dir(pattern = "10m.*\\.tif$")
files10
image10=stack(files10)

#Downscale 20m resolution bands: Using raster package function
disaggregate
files20= dir(pattern = "20m.*\\.tif$")
files20

image20=stack(files20)
image20d= disaggregate(image20, fact=2)
image20d

#Join image stacks
image=stack(image10,image20d)
image
```

```
# import LUCAS data
p=readOGR("C:/Users/Daria/Desktop/Thesis/Points","p3")

p$SURVEY_LC1
table(p$SURVEY_LC1)

# reclassify LUCAS to Austrian nomenclature
a=which(p$SURVEY_LC1==c("A11")|p$SURVEY_LC1==c("A21")|p$SURVEY_LC1==
c("A22"))
p@data[a,"austria"]="1"

b=which(p$SURVEY_LC1==c("F10")|p$SURVEY_LC1==c("F20")|p$SURVEY_LC1==
c("F40"))
p@data[b,"austria"]="2"

c=which(p$SURVEY_LC1==c("G11")|p$SURVEY_LC1==c("G21"))
p@data[c,"austria"]="3"

d=which(p$SURVEY_LC1==c("C10")|p$SURVEY_LC1==c("C22")|p$SURVEY_LC1==
c("C32")|p$SURVEY_LC1==c("C33")|p$SURVEY_LC1==c("D10")|p$SURVEY_LC1=
=c("D20")|p$SURVEY_LC1==c("B71")|p$SURVEY_LC1==c("B72")|p$SURVEY_LC1
==c("B73")|p$SURVEY_LC1==c("B74")|p$SURVEY_LC1==c("B75")|p$SURVEY_LC
1==c("B76")|p$SURVEY_LC1==c("B81")|p$SURVEY_LC1==c("B82")|p$SURVEY_L
C1==c("B83")|p$SURVEY_LC1==c("Bx2"))
p@data[d,"austria"]="4"

e=which(p$SURVEY_LC1==c("E10")|p$SURVEY_LC1==c("E20")|p$SURVEY_LC1==
c("E30"))
p@data[e,"austria"]="5"

f=which(p$SURVEY_LC1==c("B11")|p$SURVEY_LC1==c("B12")|p$SURVEY_LC1==
c("B15")|p$SURVEY_LC1==c("B16")|p$SURVEY_LC1==c("B17")|p$SURVEY_LC1=
=c("B18")|p$SURVEY_LC1==c("B19")|p$SURVEY_LC1==c("B21")|p$SURVEY_LC1
==c("B31")|p$SURVEY_LC1==c("B42")|p$SURVEY_LC1==c("B43")|p$SURVEY_LC
1==c("B53")|p$SURVEY_LC1==c("B54")|p$SURVEY_LC1==c("B55")|p$SURVEY_L
C1==c("Bx1"))
p@data[f,"austria"]="6"

table(p$austria)

# Extract pixel values to LUCAS points
values =extract(image,p)

# randomForest
ctrl = trainControl(method = "repeatedcv",repeats = 2)
randomForest.fit=train(x=values, y=p$austria, method="rf",
ntree=500,tuneLength=10,trControl=ctrl,summaryFunction = TRUE)
# see fucntion 'randomForest' in package randomForest
plot(randomForest.fit)
save.image("C:/Users/Daria/Desktop/Thesis/tiffs/all.RD")

# image classification
time1=Sys.time()
```

```
map=predict(image,randomForest.fit)
Sys.time()-time1
plot(map)
writeRaster(map,"map.tif",datatype="INT1U",overwrite=TRUE)
save.image("C:/Users/Daria/Desktop/Thesis/tiffs/all.RData")
```

4. Code for Classification based on Original LUCAS Data

```
# settings
#install.packages()
library(raster)
library(rgdal)
library(caret)
library(e1071)
library(randomForest)

setwd("C:/Users/Daria/Desktop/2.06/tiffs")

getwd()

# import 10m TIFF images
files10=dir(pattern = "10m.*\\.tif$")
files10
image10=stack(files10)

#Downscale 20m resolution bands: Using raster package function
disaggregate
files20= dir(pattern = "20m.*\\.tif$")
files20

image20=stack(files20)
image20d= disaggregate(image20, fact=2)
image20d

#Join image stacks
image=stack(image10,image20d)
image

# import LUCAS data
p=readOGR("C:/Users/Daria/Desktop/2.06/tiffs","PT_2015_20160921")
p=crop(p,image)
#plot(image[[1]])
#plot(p,add=T)

p$SURVEY_LC1
table(p$SURVEY_LC1)

#eliminate empty classes of land cover class labels- not necessary
when pre-cropping in Arc
p$SURVEY_LC1=droplevels(p$SURVEY_LC1)
table(p$SURVEY_LC1)

#Drop H21 class
```

```
g=which(!p$SURVEY_LC1==c("H21"))
p@data[g,"austria"]="0"
p=p[g,]

# reclassify LUCAS to Austrian nomenclature
a=which(p$SURVEY_LC1==c("A11")|p$SURVEY_LC1==c("A21")|p$SURVEY_LC1==
c("A22"))
p@data[a,"austria"]="1"

b=which(p$SURVEY_LC1==c("F10")|p$SURVEY_LC1==c("F20")|p$SURVEY_LC1==
c("F40"))
p@data[b,"austria"]="2"

c=which(p$SURVEY_LC1==c("G11")|p$SURVEY_LC1==c("G21"))
p@data[c,"austria"]="3"

d=which(p$SURVEY_LC1==c("C10")|p$SURVEY_LC1==c("C22")|p$SURVEY_LC1==
c("C32")|p$SURVEY_LC1==c("C33")|p$SURVEY_LC1==c("D10")|p$SURVEY_LC1=
=c("D20")|p$SURVEY_LC1==c("B71")|p$SURVEY_LC1==c("B72")|p$SURVEY_LC1
==c("B73")|p$SURVEY_LC1==c("B74")|p$SURVEY_LC1==c("B75")|p$SURVEY_LC
1==c("B76")|p$SURVEY_LC1==c("B81")|p$SURVEY_LC1==c("B82")|p$SURVEY_L
C1==c("B83")|p$SURVEY_LC1==c("Bx2"))
p@data[d,"austria"]="4"

e=which(p$SURVEY_LC1==c("E10")|p$SURVEY_LC1==c("E20")|p$SURVEY_LC1==
c("E30"))
p@data[e,"austria"]="5"

f=which(p$SURVEY_LC1==c("B11")|p$SURVEY_LC1==c("B12")|p$SURVEY_LC1==
c("B15")|p$SURVEY_LC1==c("B16")|p$SURVEY_LC1==c("B17")|p$SURVEY_LC1=
=c("B18")|p$SURVEY_LC1==c("B19")|p$SURVEY_LC1==c("B21")|p$SURVEY_LC1
==c("B31")|p$SURVEY_LC1==c("B42")|p$SURVEY_LC1==c("B43")|p$SURVEY_LC
1==c("B53")|p$SURVEY_LC1==c("B54")|p$SURVEY_LC1==c("B55")|p$SURVEY_L
C1==c("Bx1"))
p@data[f,"austria"]="6"

table(p$austria)


# Extract pixel values to LUCAS points
values =extract(image,p)

# randomForest
ctrl = trainControl(method = "repeatedcv",repeats = 2)
randomForest.fit=train(x=values, y=p$austria, method="rf",
ntree=500,tuneLength=10,trControl=ctrl,summaryFunction = TRUE)
# see fucntion 'randomForest' in package randomForest
plot(randomForest.fit)


# image classification
time1=Sys.time()
map=predict(image,randomForest.fit)
Sys.time()-time1
```

```
plot(map)
writeRaster(map,"mapLUCAS.tif",datatype="INT1U",overwrite=TRUE)
```

5. Code for Accuracy Assessment

```
#install.packages()
library(raster)
library(rgdal)
library(caret)
library(lulcc)

#load maps
maps=raster("maps.tif")
maps
s5=raster("s5.tif")
s5
ss859=raster("map859.tif")
ss859
ss880=raster("map880.tif")
ss880
luc=raster("mapLUCAS.tif")
luc

#load accuracy assessment points
p<-readOGR("C:/Users/Daria/Desktop/AA","AAP2lim_corrected")
p$SURVEY_LC1
a<-which(p$SURVEY_LC1==c("A11"))
p@data[a,"austria"]<-"1"

b<-which(p$SURVEY_LC1==c("F40"))
p@data[b,"austria"]<-"2"

c<-which(p$SURVEY_LC1==c("G11"))
p@data[c,"austria"]<-"3"

d<-which(p$SURVEY_LC1==c("D10"))
p@data[d,"austria"]<-"4"

e<-which(p$SURVEY_LC1==c("E10"))
p@data[e,"austria"]<-"5"

f<-which(p$SURVEY_LC1==c("B11"))
p@data[f,"austria"]<-"6"

table(p$austria)


#extract values for AAP locations
values <-extract(maps,p)
table(values)

values2 <-extract(s5,p)
table(values2)
```

```r
values3 <-extract(ss859,p)
table(values3)

values4 <-extract(ss880,p)
table(values4)

values5 <-extract(luc,p)
table(values5)

#create data frame from values

df=data.frame(values,p$austria)

conf_mat_tab1 <- table(lapply(df, factor, levels = seq(1, 6, 1)))
confusionMatrix(conf_mat_tab1)

#User Accuracy
diag(conf_mat_tab1) /rowSums(conf_mat_tab1)
#Producer Accuracy
diag(conf_mat_tab1) /colSums(conf_mat_tab1)

df2=data.frame(values2,p$austria)

conf_mat_tab2 <- table(lapply(df2, factor, levels = seq(1, 6, 1)))
confusionMatrix(conf_mat_tab2)

#User Accuracy
diag(conf_mat_tab2) /rowSums(conf_mat_tab2)
#Producer Accuracy
diag(conf_mat_tab2) /colSums(conf_mat_tab2)


df3=data.frame(values3,p$austria)

conf_mat_tab3 <- table(lapply(df3, factor, levels = seq(1, 6, 1)))
confusionMatrix(conf_mat_tab3)

#User Accuracy
diag(conf_mat_tab3) /rowSums(conf_mat_tab3)
#Producer Accuracy
diag(conf_mat_tab3) /colSums(conf_mat_tab3)

df4=data.frame(values4,p$austria)

conf_mat_tab4 <- table(lapply(df4, factor, levels = seq(1, 6, 1)))
confusionMatrix(conf_mat_tab4)

#User Accuracy
diag(conf_mat_tab4) /rowSums(conf_mat_tab4)
#Producer Accuracy
diag(conf_mat_tab4) /colSums(conf_mat_tab4)

df5=data.frame(values5,p$austria)
```

```
conf_mat_tab5 <- table(lapply(df5, factor, levels = seq(1, 6, 1)))
confusionMatrix(conf_mat_tab5)

#User Accuracy
diag(conf_mat_tab5) /rowSums(conf_mat_tab5)
#Producer Accuracy
diag(conf_mat_tab5) /colSums(conf_mat_tab5)
```